

Dynamics of Rotation of Super-Earths

N. CALLEGARI JR. and A. RODRÍGUEZ

the date of receipt and acceptance should be inserted later

Abstract We numerically investigate the dynamics of rotation of several close-in terrestrial exoplanets candidates. In our model, the rotation of the planet is disturbed by the torque of the central star due to the asymmetric equilibrium figure of the planet. We use surfaces of section and spectral analysis to explore numerically the rotation phase space of the systems adopting different sets of parameters and initial conditions close to the main spin-orbit resonant states. We show that, depending on some parameters of the system like the radius and mass of the planet, orbital eccentricity etc, the rotation can be strongly perturbed and a chaotic layer around the synchronous state may occupy a significant region of the phase space. 55 Cnc e is an example.

Keywords Celestial Mechanics · Terrestrial Exoplanets · Spin-Orbit resonances

1 Introduction

1.1 Motivation

Several works on physics of exoplanets assume an equilibrium state for the rotation of the planet. Following we give a brief list of references of different kind of studies on exoplanets which suppose in their models that the planet is tidally locked: Measurement of the rotation and oblateness of transiting giant exoplanets (e.g. Seager and Hui 2002; Barnes et al. 2003; Carter and Winn 2010); Generation of magnetic fields in exoplanets (e.g. Zuluaga and Cuartas-Restrepo 2012; see also

N. CALLEGARI JR.

Instituto de Geociências e Ciências Exatas, Unesp - Univ Estadual Paulista, Av. 24-A, 1515, CEP 13506-900, Rio Claro/SP/Brazil.

Tel.: 55-19-3526-9132

E-mail: calleg@rc.unesp.br

A. RODRÍGUEZ

Departamento de Astronomia, Instituto de Astronomia, Geofísica e Ciências Atmosféricas - Universidade de São Paulo, Rua do Matão, 1226, CEP 05508-090, São Paulo/SP/Brazil.

Tel.: 55-11-3091-2704

E-mail: adrian@astro.iag.usp.br

Lammer et al. 2009 and references therein); Atmosphere and climate of exoplanets (e.g. Lammer et al. 2008, Dobrovolskis 2007, Dobrovolskis 2009, Showman and Polvani 2011, Castan and Menon 2011); Secular orbital evolution due to tidal effects (e.g. Jackson et al. 2008a; Rodríguez et al. 2011); Tidal heating (e.g. Levrard et al. 2007, Wisdom 2008, Jackson et al. 2008b,c); Interior structure of exoplanets (e.g. Ragozzine and Wolf 2009, Batygin et al. 2009; Kramm et al. 2011).

It is well known that the detected exoplanets have in general unusual orbits when compared to the Solar System's planets. For instance, many planets are much closer to their stars than Mercury is to the Sun. Some of these planets, the so-called close-in planets, have also eccentric orbits (see Table I). Thus, we can ask if the strength of the torque of the star in their rotational motion may be important. The main task here is to investigate this question. There exist in literature several studies on the global dynamics of rotation of fictitious exoplanets which explore analytically and/or numerically the rotation phase space (e.g. Kitiashvili and Alexander 2008, Celletti and Voyatzis 2010). Our contribution here is to give details on the dynamics of rotation and stability of several known Earth-like candidates, in the vicinity of the synchronism and other spin-orbit resonant states.

In this work we focus the attention in the conservative model, where we do not investigate the effects on the spin rate of the planet due to dissipative forces, like those associated to tides. Therefore we consider here only the gravitational torque due to the non-sphericity of the planet figure. However, our investigation can be useful in the interpretation of results in which tidal forces are taken into account in the rotational history of the planet rotation (e.g. Rodríguez et al. 2012).

1.2 The model

Several aspects of the physics of rotation of close-in exoplanets can be understood with the 1.5-degree-of-freedom dynamical system often applied in studies of physical libration in rotation of regular satellites of the Solar system, the Moon and Mercury (e.g. Goldreich and Peale 1966):

$$\ddot{\theta} = \frac{3}{2} \left(\frac{B-A}{C} \right) \frac{Gm_0}{r^3} \sin 2(f - \theta), \quad (1)$$

$$\dot{f} = \frac{\sqrt{G(m_0 + m)a(1 - e^2)}}{r^2}, \quad r = \frac{a(1 - e^2)}{1 + e \cos f}, \quad (2)$$

where: θ is an angle measured from an inertial line, G is the gravitational constant; m_0 , m are the masses of the central star and the planet, respectively; $A < B < C$ are the principal moments of inertia; a , e , f are the semi-major axis, eccentricity and true anomaly, respectively. It is assumed non-circular (elliptical) shape of the equator of the planet and null obliquity. Therefore, in the model, the rate of rotation of the secondary body is disturbed by the torque of the star on the non-spherical shape of the planet. We consider the two-body problem approximation for the motion of the system¹ so that the mutual perturbations between the bodies belonging to multiple systems (see Section 1.4) are neglected in this paper.

¹ In this work we consider the case of prograde orbits and rotation. However, exoplanets in retrograde orbits with respect to the rotation axis of the star have been detected (e.g.

A basic assumption in the application of the model (1) is that the planet has a permanent quadrupole structure. Examples of bodies with this physical property in the solar system are the terrestrial planets and the regular satellites, all of which are, in spite of the details of their interior structures, solid-like bodies. In the case of exoplanets, CoRoT-7b, Kepler-10b and 55 Cnc-e are examples of probably solid-like Super-Earths (Léger et al. 2009, Batalha et al. 2011, Valencia 2011, Gillon et al. 2012). They are transiting planets which physical parameters are being studied in several works. For instance, the mass of CoRoT-7b has been estimated by several teams obtaining different results (see Ferraz-Mello et al. 2011).

It is still difficult to be sure about the structure of probably Earth-like exoplanets at the current status (see Valencia 2011, Léger et al. 2011, for the case of CoRoT-7b). In the case of exoplanets, the actual knowledge on planetary structure have suffered important developments (see Baraffe et al. 2010, Valencia 2011, Léger et al. 2011, and references therein). In particular, Valencia et al. (2007a) show that, for a determined value of the mass of a rock planet in the interval $m < 10M_E$ (M_E is the Earth mass), its radius must be smaller than a determined value which depends on m . The limits of the radius for a given mass are the following: 6600; 8600; 10,440; 11,600 and 12,200 km for 1, 2.5, 5, 7.5 and 10 M_E , respectively. So, if a planet with $m < 10M_E$ has a radius larger than its corresponding value in the above interval, its composition can have important quantities of material with density smaller than the rock material, like water for instance. In that cases a permanent deformation is not, in principle, guaranteed. In the same sense Hot-Jupiters, similarly to the cases of the solar system's jovian planets, are probably composed mainly of gas and we also do not include them in this study because additional discussions are necessary in order to consider a fixed structure for these bodies (see Levrard et al. 2007, Rodríguez et al. 2012).

Our main goal in this work, i.e., the application of the model (1) for solid-like planets, has a main limitation: the total ignorance of the quantity $\frac{B-A}{C}$ which appears in the amplitude of the perturbation of the planet rotation. In Section 2 we propose a method to estimate the value of $\frac{B-A}{C}$ of Super-Earths with known values of radius and mass. In Section 2 we also show how to infer $\frac{B-A}{C}$ as a function of several parameters (e.g., mass, distance, radius etc) of systems whose planets do not have transiting measurement and therefore do not have a determination of the radius of the planet.

1.3 Methodology

Wisdom et al. (1984) study solutions of the Equations (1,2) through the computation of surfaces of sections. They numerically show the possibility of chaotic rotation around the synchronous and other spin-orbit states for non-spherical satellites orbiting their planets in compact and eccentric orbits. We use the Wisdom's methodology and apply it in the rotation dynamics of exoplanets. In Section 3 we show the main results of numeric integrations of Equations (1,2) for several planets listed in Table I. In some cases we compare the results obtained with surfaces

Hébrard et al. 2011, and references therein). Retrograde rotation is also a possible equilibrium state (Correia et al. 2008). The study of spin-orbit resonances in retrograde motion should be interesting.

of section with dynamical maps based in spectral analysis of the solutions (e.g. Michtchenko and Ferraz-Mello 2001).

Our simulations cover wide ranges of the free parameters including moments of inertia ratio and orbital eccentricity. We also give the range of some other parameters (like planetary radius, mass) which would correspond to solid-like planets in view of structure models of exoplanets (e.g. Valencia 2007a,b; 2011). Thus, we discuss the dynamics of planetary rotation with our model in large sets of initial conditions and appropriate parameters corresponding to solid-like planets. We consider planets with orbital period $P < 33$ days and mass $m < 15M_E$. Table I shows the data of several Super-Earths considered here. Inspection of Table I helps us to see some common properties of all planets which we study here. For instance, there are several planets with published value of non-circular orbit, even with very small values of orbital period $P < 7days$. As we see in Appendix A (see below), the existence of non-circular orbits for close-in planets is in conflict with the classical results of orbital circularization of close-in orbits due to tidal effects.

1.4 Orbital eccentricity

As we will see in Section 3, the planets with more rich rotational dynamics are those which move in eccentric orbits. In fact, the planet's orbital eccentricity plays an important role since in the case of non-circular orbit the amplitude and argument of the sine in (1) suffer temporal variation. However, the existence of eccentric close-in orbits in single-planet systems cannot be guaranteed. In fact, an initial eccentric orbit would be tidally damped, evolving to circularization in timescales depending on physical parameters of the interacting pair and also on the initial values of the elements (see Dobbs-Dixon et al. 2004, Ferraz-Mello et al. 2008, Rodríguez and Ferraz-Mello 2010, Rodríguez 2010). In Appendix A we calculate, using averaged equations, the circularization timescale of the Super-Earth CoRoT-7b, adopting different dissipative parameters. Our results, in agreement with previous ones, show that tidal evolution of systems with close-in companions with orbital period less than one week can be the responsible for the circularization of the orbits.

Thus, probably the values of the eccentricities of some close-in *single-planets* listed in Table I are not well determined by the current methods of orbital fitting, and/or some additional mechanism can explain the non-null values. For instance, under the hypothesis of an additional undetected resonant companion, a large value of eccentricity of a single planet can be in fact close to zero, a result that shows a degeneracy of the problem of orbital determination of the system (Anglada-Escudé et al. 2010). Tadeu dos Santos et al. (2012), in a paper written with the main propose of study the dynamics and the determination of the orbital elements of Gl 581g, show degeneracy in the determination of the eccentricity of all members of the Gl 581 system. In this case, degeneracy means that depending on the planetary architecture adopted in the model (e.g. number of planets), different solutions are possible with the same statistical significance for different values of eccentricity.

The existence of exterior companions can also work as a dynamical mechanism which may explain the non-null eccentricity values of close-in planets of *multi-planetary* systems. Spiegel et al. (2010) evaluate that terrestrial planets at 1 AU can be highly perturbed by an outer giant planet, which may excite large variations of eccentricity of the inner planet. At such distances, however, tidal effects may be

negligible (Appendix A), and eccentricity may be large. However, previous works have show that, the combination of secular interaction and tides raised on the inner planet by the star result in the circularization of both orbits (see Mardling 2007; Rodríguez et al. 2011). Indeed, depending on the planet mass ratio, the perturbation of the companion acts to increase the circularization timescale of the inner orbit. Hence, the explanation for the non-null eccentricities of close-in planets remains under discussion (see Matsumura et al. 2008, Correia et al. 2010, Correia et al. 2012).

Therefore, notwithstanding all the above discussions, we consider in this work the orbital eccentricity as an open parameter in our calculations. The reported values, listed in Table I with the error bars, will also be taken into account for sake of reference.

Table I: Data of planets with orbital period $P < 33days$ (except Kepler-11f) and mass $m < 15M_E$, where M_E is the Earth mass. The list is sorted in increasing value of the orbital period. The data have been taken from <http://exoplanet.eu/index.php> except in other cases indicated. The other units are the solar mass (M_{SUN}) and the Astronomical Unit (AU). ^a: Ferraz-Mello et al. (2011); ^b: Planet present in multiple system; ^c: See also Section 3.2.1. ^d: Value taken from Charpinet et al. (2011), differing from the value given in <http://exoplanet.eu/index.php>.

Planet	m : Mass (M_E)	m_0 : Star's mass (M_{SUN})	P : Orbital Period (day)	a : semi-major axis (AU)	e : eccentricity
KOI-55b	0.445 ^d	0.496	0.2401	0.006	? ^b
KOI-961c	1.907	0.13	0.4533	0.006	? ^b
KOI-55c	0.667	0.496	0.3429	0.0076	? ^b
55 Cnc e	8.58	0.905	0.7365	0.0156	$< 0.06^b$
Kepler-10b	4.55	0.895	0.8375	0.0168	0 ^b
CoRoT-7b	8.5 ^a	0.93	0.8536	0.0172	0 ^b
KOI-961b	2.8604	0.13	1.2138	0.0116	? ^b
GJ 1214b	6.357	0.153	1.58	0.014	< 0.27
Kepler-9d	6.99	1.0	1.5928	0.0273	? ^b
KOI-961d	0.9535	0.13	1.8516	0.0154	? ^b
GJ 876d	6.67	0.334	1.9378	0.02	$0.207 \pm 0.05^{b,c}$
GJ 3634b	7.0	0.45	2.6456	0.0287	0.08 ± 0.057
Kepler-21b	< 10.488	1.34	2.7857	0.0425	0
Kepler-18b	6.897	0.972	3.5047	0.0447	0 ^b
Kepler-20b	8.58141	0.912	3.6961	0.0454	$< 0.320^b$
CoRoT-7c	8.39	0.93	3.698	0.046	0 ^b
HD 156668b	4.16	0.772	4.646	0.05	0
GJ 674b	11.76	0.35	4.6938	0.039	0.2 ± 0.02
HD 7924b	9.217	0.832	5.3978	0.057	0.17 ± 0.16
HD 45184b	12.7132	-	5.8872	0.0638	0.3
Kepler-20e	< 3.083	0.912	6.0985	0.0507	? ^b
GJ 176b	8.42	0.49	8.7836	0.066	0
HD 97658b	6.356	0.85	9.4957	0.0797	0.13 ± 0.06
HD 125595b	14.30	0.76	9.67	0.078	0
Kepler-11b	4.3	0.95	10.3037	0.091	0 ^b
Kepler-11c	13.507	0.95	13.025	0.106	0 ^b
Kepler-20f	14.3	0.912	19.577	0.11	? ^b
Kepler-11d	6.099	0.95	22.687	0.159	0 ^b
Kepler-11e	8.40	0.95	31.9959	0.194	0 ^b
Kepler-11f	2.3	0.95	46.6888	0.25	0 ^b

2 The Prolateness

The first quantity which we must have in hand in order to study the system (1-2) is the ratio $\frac{B-A}{C}$. Here we propose a method to estimate the value of $\frac{B-A}{C}$ as a function of several parameters of the system, like the mass of the star, the mass of the planet, the semi-major axis, and the radius of the planet.

Consider a homogeneous *non-viscous*² rotating planet orbiting a star. The equilibrium figure of a rotating body (with axes a , b and c) under the action of the tide generating force of the central star, lying in the equatorial body's plane, is given by a Roche ellipsoid in which $a > b > c$ (see Chandrasekhar 1969). The smaller axis is perpendicular to the largest axis, which is pointed in the direction of the central body in the case of synchronous rotation. In this case, we have the following expression for the deformation of the equator, or the *prolateness*, hereafter denoted by ϵ :

$$\epsilon = \frac{a-b}{a} = \frac{15}{4} \frac{m_0}{m} \left(\frac{R}{r}\right)^3 \left(1 - \frac{5(m_0+m)}{2m} \left(\frac{\Omega}{n}\right)^2 \left(\frac{R}{r}\right)^3\right)^{-1} \quad (3)$$

(e.g. Ferraz-Mello et al. 2008).

When the rotation is neglected, the attained equilibrium figure is a Jeans spheroid with $b = c$. In this case, the value of ϵ is given by equation above without the second term. A classical result shows that for a free synchronous rotating body the polar deformation or oblateness (that is, $1 - \frac{c}{b}$) is three times smaller than the prolateness due to the companion (when rotation is neglected, see Danby 1988, p.121). The restriction $b = c$ enable us to write ϵ in a convenient form. Indeed, the momenta of inertia of the spheroid can be written as

$$A = \frac{1}{5}m(b^2 + c^2), \quad B = \frac{1}{5}m(a^2 + c^2), \quad C = \frac{1}{5}m(a^2 + b^2). \quad (4)$$

Hence, using the definition of ϵ and imposing $b = c$ into above equations we arrive to

$$\frac{A}{C} = \frac{2}{(1-\epsilon)^{-2} + 1} \simeq 1 - \epsilon - \frac{1}{2}\epsilon^2. \quad (5)$$

Therefore, at first order in ϵ :

$$\frac{B-A}{C} \simeq \epsilon. \quad (6)$$

Contrary to the case of some bodies of the Solar system³, the values of the momenta of inertia of exoplanets are completely unknown quantities. However, we can take an idea of the magnitude of the prolateness by using equations (3) and (6).

² In this hypothesis we are neglecting the dynamic tidal torque raised by the central star which also affect the planet rotation. However, several planets which we study here are so close to their star that tidal effects may be important, mainly in the case of eccentric orbits. We devoted to Appendix B the illustration of one case in which the tidal torque is taken into account and applied to CoRoT-7b super-Earth planet.

³ In order to test the validity of Equation (6) we estimate ϵ for some bodies of the Solar System. For Europa we estimate $\epsilon \sim 1.9 \times 10^{-3}$, a value for which the order of magnitude agrees with current estimative of $\sim 1.5 \times 10^{-3}$. The latter value has been obtained from the numerical values of the gravitational coefficient C_{22} and mean moment of inertia $\xi = \frac{C}{mR^2}$ given in Van Hoolst et al. (2008) through the relation $\epsilon = 4C_{22}/\xi$. In the case of Titan, we obtain $C_{22} = 1.4 \times 10^{-5}$, in agreement with one reported value of about 1×10^{-5} (Iess et al. 2010). For Io, we find $C_{22} = 3.4 \times 10^{-4}$, in concordance with Schubert et al. (2004), who reported $C_{22} = 5.6 \times 10^{-4}$. For Mercury we obtain $\epsilon \sim 10^{-6}$, while its current order of magnitude is $\sim 10^{-4}$. Mercury has an eccentric orbit (0.205), but our estimative of ϵ does not change considering Mercury at the pericenter. Probably the dependence of ϵ on the eccentricity and distance be more complex in the case of more distant and eccentric planets.

The dependence on $\left(\frac{\Omega}{n}\right)^2$ in (3) is in fact weak. For instance, Table II shows the values of ϵ considering $\Omega = n$ for several transiting Super-Earths which has a determination of the radius. In the case of 55 Cnc e, $\epsilon \sim 2.8 \times 10^{-2}$. For $\Omega = 2n$, $\epsilon \sim 2.97 \times 10^{-2}$. If we neglect the rotation term and consider $\Omega = 0$, we have $\epsilon \sim 2.75 \times 10^{-2}$. These values are smaller than when the uncertain in radius of planet is considered in the calculation of ϵ . For instance, in the case of 55 Cnc e, Gillon et al. (2012) give $R = 2.17 \pm 0.10 R_E$, which results the maximum values: $\epsilon \sim 3.21 \times 10^{-2}$ ($\Omega = n$), $\epsilon \sim 3.43 \times 10^{-2}$ ($\Omega = 2n$), $\epsilon \sim 3.14 \times 10^{-2}$ ($\Omega = 0$).

All other planets listed in Table I do not have an estimative for R . In these cases we can estimate the order of magnitude of ϵ by analyzing its dependence with different parameters, as we illustrate below. Figures 1(a-e) show the level curves of the function $\epsilon = \epsilon(r, m)$ calculated with Equation (3) considering five fixed values of the radius of a fictitious planet of a star with mass $m_0 = 1m_{SUN}$, where m_{SUN} is the solar mass. The contours given in gray color correspond to “small” value of $\epsilon < 0.01$, while the colored levels correspond to “large” prolateness where $\epsilon \geq 0.01$. We arbitrarily define here the value $\epsilon = 0.01$ as the limit between large and small prolateness of Super-Earths⁴. Figure 1(a) shows that exoplanets similar to the Earth (i.e., with mass and radius similar to the Earth’s values) can have large equatorial prolateness for all $r < 0.018AU$ (note the colored level curves near to the bottom left of the panel).

A zoom close to the origin of the Figure 1(a) is shown in Figure 1(f). We can note that for small values of (r, m) in the figure we have $\epsilon \sim 1$ (blue levels)⁵. Thus Figure 1(f) suggests that a planet with $r \ll 0.018$ can suffer important effects of the torque on its rotation. The recently discovered members of the planetary system of the stars KOI-961 and KOI-55 are examples of such kind of planets orbiting sub solar mass stars (see Table I). As they are transiting planets we can calculate their ϵ . Table II shows that the prolateness of KOI-55b, KOI-55c and KOI-961c are large, i.e., $\epsilon > 0.01$ while in the case of KOI-961b,d, $\epsilon < 0.01$. In Section 3.1.2 we will study the rotational dynamics of these planets in details.

Finally we note that in the present study we have assumed constant $\frac{B-A}{C}$ value. However, depending on the adjustment to hydrostatic equilibrium $\frac{B-A}{C}$ may be itself time-dependent. The time-scale for adjustment to the completely relaxed state depends on material parameters, e.g., rigidity and viscosity which are highly temperature dependent. Furthermore, it will depend on the spin-orbit coupling the planet is trapped in. For the application to terrestrial planets given here the constant, i.e. frozen, $\frac{B-A}{C}$ configuration is justified because adjustment of solid rocky planets to equilibrium usually occurs on geological time-scales. Therefore, the states described here do not necessarily represent hydrostatic configurations. For Jupiter-like planets the simplification of constant $\frac{B-A}{C}$ values may not be justified because of the fluid behavior of the gas giants even on the short time-scales of their orbital periods. Adjustment to the hydrostatic state in a specific resonance will be relatively fast. In this case the time-dependence of the gas giants $\frac{B-A}{C}$ must be taken into account in a coupled set of differential equations describing the spin, the orbit and the hydrostatic gravity field of the planet.

⁴ As we will see in details in Section 3, for $\epsilon > 0.01$ the rotation may be highly disturbed by the torque of the central star in the case of eccentric orbits. However, this division between “small” and “large” prolateness is arbitrary and will be used in this work only for didactic purposes.

⁵ We remark that very large values of ϵ close to the unit are not valid within the first-order approximation in ϵ .

Table II: Numerical value of $\frac{B-A}{C} \simeq \epsilon$ (Equation (1)) for several Super-Earths with known radius. ϵ has been calculated with Equation (3) where we consider $\Omega = n$. The values of radius, in units of the Earth radius ($1R_E = 6,378$ km), have been taken from <http://exoplanet.eu/index.php>. ^a: Charpinet et al. (2011); ^b: The current estimative in <http://exoplanet.eu/index.php> is $2.84 \pm 0.2 R_E$; ^c This value differs from those given in Version 1 (v1) ($\epsilon = 0.117$) because we use the mass of the planet given in Charpinet et al. (2011), which is ten times smaller than the value given in <http://exoplanet.eu/index.php>.

Planet	$\frac{B-A}{C}$	$R (R_E)$
KOI-55b ^c	2.60×10^{-1}	0.76^a
KOI-55c	1.17×10^{-1}	0.87^a
55 Cnc e	2.80×10^{-2}	$2.17^{+0.1}_{-0.1}$
GJ 1214b	1.77×10^{-2}	2.74^b
KOI-961c	1.18×10^{-2}	$0.73^{+0.2}_{-0.2}$
Kepler-10b	1.15×10^{-2}	$1.42^{+0.033}_{-0.036}$
CoRoT-7b	9.92×10^{-3}	$1.68^{+0.09}_{-0.09}$
Kepler-9d	3.04×10^{-3}	$1.64^{+0.19}_{-0.14}$
KOI-961b	1.35×10^{-3}	$0.78^{+0.22}_{-0.22}$
Kepler-18b	1.22×10^{-3}	$2.00^{+0.1}_{-0.1}$
Kepler-20b	7.56×10^{-4}	$1.90^{+0.12}_{-0.21}$
Kepler-21b	6.99×10^{-4}	$1.63^{+0.04}_{-0.04}$
KOI-961d	6.70×10^{-4}	$0.57^{+0.18}_{-0.18}$
HD 97658b	6.45×10^{-4}	$2.93^{+0.28}_{-0.28}$
Kepler-11b	2.18×10^{-4}	$1.97^{+0.19}_{-0.19}$
Kepler-11c	1.80×10^{-4}	$3.15^{+0.3}_{-0.3}$
Kepler-11d	1.52×10^{-4}	$3.43^{+0.32}_{-0.32}$
Kepler-20e	1.45×10^{-4}	$0.868^{+0.074}_{-0.096}$
Kepler-11e	1.39×10^{-4}	$4.52^{+0.43}_{-0.43}$
Kepler-11f	4.57×10^{-5}	$2.61^{+0.25}_{-0.25}$
Kepler-20f	4.72×10^{-6}	$1.00^{+0.1}_{-0.13}$

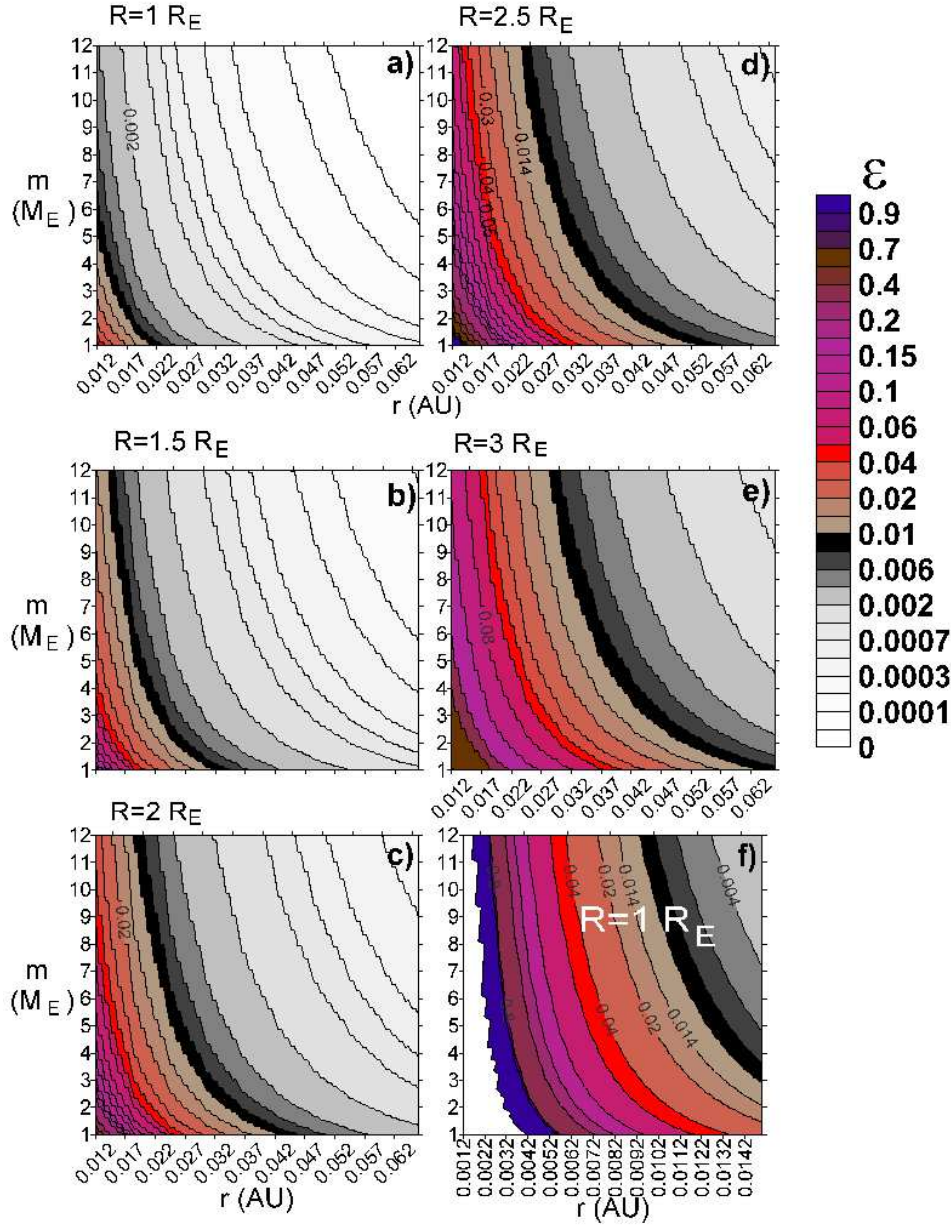


Fig. 1 (a-e) Level curves of ϵ in the plane $(r \times m)$ (star-planet distance (r) and the mass of the planet (m)), for different values of the radius of a fictitious planet orbiting a star with $1 M_{SUN}$. (f) Zoom of Figure 1(a) close to the origin of the r -axis. The blue contour shown in (f) shows prohibitive levels with $\epsilon \sim 1$. The white portion of the figure close to the origin corresponds to the levels curves which are not physically possible to exist since they correspond to $\epsilon > 1$. The units are the Earth radius (R_E), the Earth mass (M_E), the solar mass (M_{SUN}) and the Astronomical Unit (AU).

3 Surfaces of Section and the Dynamics of Rotation

In this section we show surfaces of section of the numerically computed solutions⁶ of the model (1) for several Super-Earths listed in Table I. Following Wisdom et al. (1984), we investigate the dynamics of rotation in the plane $(\theta, \dot{\theta}/n)$ at $f = 0$, where f is the true anomaly and $\dot{\theta}/n$ is the ratio between the angular rotational velocity and the mean motion. Thus, in the surfaces of section, we plot the values of $(\theta, \dot{\theta}/n)$ at the moment of the passage of the planet through the pericenter in the case of eccentric orbit.

In order to present surfaces of sections, we consider four main types of Super-Earths: planets with circular or non-circular orbit, and those which are single planets or are present in *multiple* systems. We divide the presentation of the results as follows. In Section 3.1 we review basic topics of spin-orbit resonances and study examples of close-in planets (single or not) with large equatorial prolateness and circular orbits. In Section 3.2 we study the dynamics of rotation of close-in planets present in multiple systems considering eccentric orbits with orbital period $P < 7.5$ days⁷. In Section 3.3 we analyze the cases of single planets in both, circular and eccentric orbits. In Section 3.4 we apply the Chirikov overlapping criterium to explore chaos in some systems around the domains of the 1:1 and 3:2 spin-orbit resonances.

3.1 Close-in Earth-like planets with circular orbits

3.1.1 CoRoT-7b, Kepler-10b and the basic topics of spin-orbit dynamics

Figure 2 shows surfaces of sections for CoRoT-7b and Kepler-10b, two Super-Earths very close to their host stars ($a \sim 0.017$ AU). Figure 2(a) corresponds to the case of CoRoT-7b. Since its orbit is circular, the system (1), (2) is integrable in this case and therefore we say that the dynamics of rotation of CoRoT-7b is regular, i.e., no chaotic motion is admissible in the domain of the model. We indicate in Figure 2(a) the domain of the synchronous motion located around the equilibrium point at $\theta = 0$, $\dot{\theta} = n$. The closed curves around the synchronous state show the amplitude of the physical libration of the major axis of the planet⁸ relative to the star, which motion is given quantitatively by the oscillation of the synodic angle $\psi = f - \theta$ around zero. In the section θ follows ψ since we put $f = 0$.

In Figure 2(b) we consider a fictitious non-null value for the orbital eccentricity, $e = 0.01$. In this case, the domain of other spin-orbit resonances may appear in the sections, like the 3:2 resonance for instance. In fact, it can be shown that the domains of low-order spin-orbit resonances exist in the phase space only in the case of $e \neq 0$. This can be understood as follows. The average, with respect to the mean-anomaly, of the torque of the star on the rotation of planets in circular orbits, is null for all low-order spin-orbit regimes except the synchronous one (Goldreich and Peale 1966). Thus, if the torque is null in a determined resonance, libration of the *corresponding synodic angle* is not possible. Therefore, in the case of circular orbit this is a physical explanation for the absence of resonant islands in the surfaces of section except the synchronous one.

The domain of the synchronous motion is always present in the phase space even for $e = 0$. For $e = 0$ the average torque is never null except if $B - A = 0$ or at the equilibrium point of the exact synchronism. For circular orbits the fixed point of the synchronous motion is located at $\dot{\theta} = n$ and $\theta = 0$. For $e \neq 0$, the fixed point corresponding to the equilibrium of the system is not located at $\dot{\theta} = n$ because the existence of a forced component (κ), and it is shifted compared to the case of null eccentricity. This can be seen by inspection of the

⁶ We use the code of Everhart (1986).

⁷ In the Section 4 we list the results for some planets with $7.5 < P < 33$ days.

⁸ Following classical astrodynamics texts (e.g. Danby 1988), we use in this work the term *physical* librations for those motion associated to the non-spherical shape of the secondary body. The often called *optical* librations do not require an asymmetry of the secondary since they are not associated to a disturbed rotator. For instance, the optical libration in longitude exists due to differences between a (constant) velocity of rotation and the instantaneous orbital velocity in an eccentric orbit. In the disturbed (non-spherical) case the optical libration is superposed to the forced component.

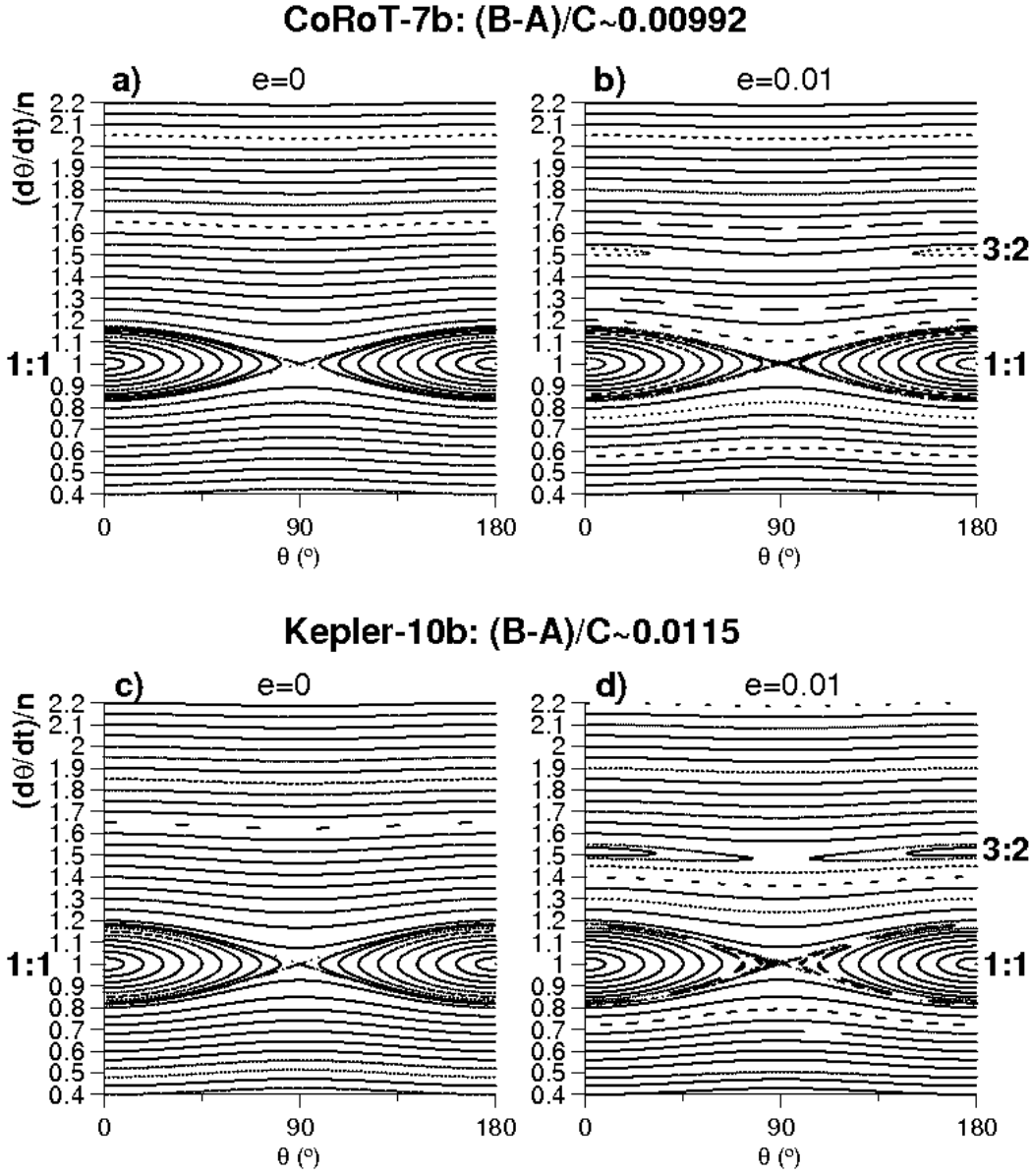


Fig. 2 Surfaces of Section in the plane $(\dot{\theta}/n \times \theta)$ of numerical solutions of (1). The sections have been done at each orbital revolution of the planets CoRoT-7b (Figures 2(a,b)) and Kepler-10b (Figures 2(c,d)). Each orbit has been integrated for 1140 orbital periods of the planet. The numerical values of $\frac{B-A}{C}$ has been calculated with Equation (3) and are given at the top of the panels (see also Table II). In the plots given at left, the orbital eccentricities correspond to the real values (i.e., the reported ones). In the plots given at right, the values of the eccentricities are fictitious and have been chosen in order to evaluate the domain of the 3:2 spin-orbit resonance in the case of quasi-circular orbit.

KOI-55c: $(B-A)/C \sim 0.117$

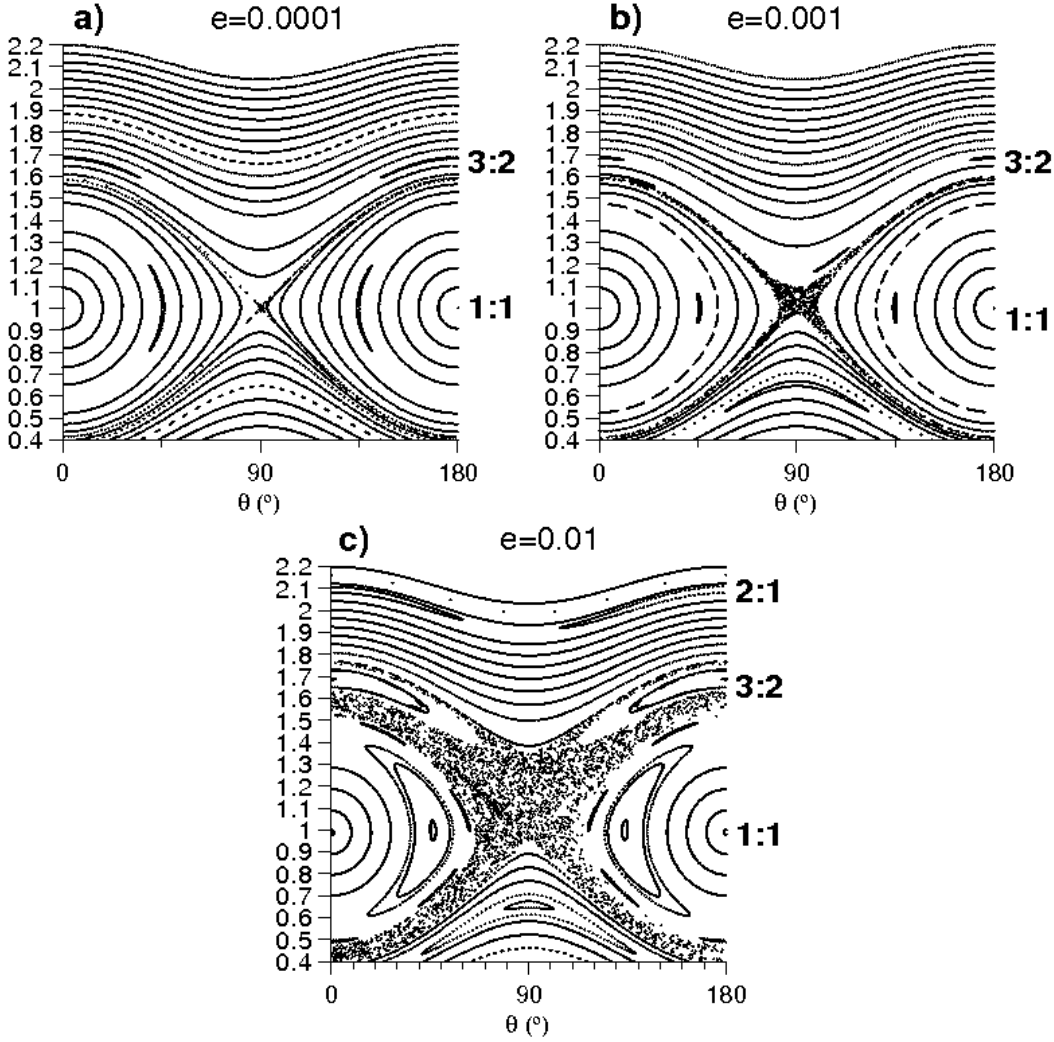


Fig. 3 Surfaces of Section in the plane $(\dot{\theta}/n \times \theta)$ of numerical solutions of (1). The sections have been done at each orbital revolution of the planet and KOI-55c. Different fictitious values of the orbital eccentricity (indicated in each plot) have been considered. Each orbit has been integrated for 1140 orbital periods of the planet. The numerical values of $\frac{B-A}{C}$ has been calculated with Equation (3) and are given at the top of the panels (see also Table II).

fixed point of the 1:1 resonance in the surfaces of sections, mainly in the case of high values of eccentricity (e.g. Figures 6(d) and 7(c,d)). At first order in eccentricity, it can be shown that: $\kappa_{1:1} \equiv \frac{2\omega_0^2}{n^2 - \omega_0^2}e$, where $\omega_0^2 = 3n^2 \frac{B-A}{C}$ for the 1:1 resonance (Murray and Dermott 1999, pages 215-16). In the surface of section, it can be shown that the equilibrium point of the 1:1 resonance is located at $\frac{\dot{\theta}}{n} \simeq 1 - \kappa$.

For small eccentricity it can be shown that physical libration of $\psi = \psi_{1:1} = f - \theta$ includes two component: the often called forced term, with frequency given by the mean-motion n , and long-term, free libration, with frequency ω_0 . The general expression of ω_0 is given by $\omega_0^2 = 3n^2 |H(p, e)| \frac{B-A}{C}$, where: $H(p, e)$ are the coefficient of the mean torque at the resonance of order p ; p is a half-integer which defines the resonance such that $p = 1$ for 1:1 resonance, $p = 2$ for 2:1, $p = +3/2$ for 3:2 etc (see Appendix B and Appendix in Rodríguez et al. 2012)⁹. For 55 Cnc e, close to the 1:1 fixed point, the long-term period is about 2.54 days, while the forced component librates at each ~ 0.736 days. In the case of non-circular orbits, chaotic rotation is physically possible mainly close to the separatrices of the spin-orbit resonances. This regime of motion is possible since the physical libration can become unstable for large amplitude. In the example given in Figure 2(b), however, the values of eccentricity and $\frac{B-A}{C}$ are very small, and the chaotic layer is very thin.

Figures 2(c,d) show the case of Kepler-10 b. We can note the similarities with the system of CoRoT-7b discussed above.

3.1.2 KOI-55b, KOI-55c

In spite of regular motion analyzed in Figure 2, we can ask if a fictitious planet closer to its star than CoRoT-7b and Kepler 10-b would have similar properties of the rotation phase space even in the case of near-circular orbits. As discussed in Section 2, depending on the star-planet distance, a planet can admit very large value of $\epsilon \gg 0.01$. We give two examples of this kind of Earth-like candidates recently discovered: KOI-55b,c, located at 0.0060 AU (planet b) and 0.0076 AU (planet c) from the star, respectively (Table I). The values estimated for $\frac{B-A}{C}$ are ~ 0.26 (KOI-55b) and ~ 0.117 (KOI-55c) (Table II).

Figure 3 shows surfaces of section for KOI-55c. The numerical values of the orbital eccentricity is unknown (Charpinet et al. 2011). Due to their proximities to the star, it can be expected that its eccentricity is close to zero (see Appendix A). However, we consider in Figure 3 three different quasi-circular orbit. The domain of the 1:1 resonance is very large. The phase space shows the presence of other spin-orbit resonances, like the 3:2 resonance. The fixed points of all resonances but the synchronous one are slightly forced from the exact commensurability. For instance, in Figure 4(a) we show the physical libration of $\psi_{3/2} = 2f - 3\theta$ adopting an initial condition within the 3:2 resonance indicated in Figure 3(b), where $\dot{\theta}_0 = 1.685n$ and not $\dot{\theta}_0 = 1.5n$ as would be expected.

The phase space also shows secondary resonances within the synchronous island. Secondary resonances occur when the period of libration of the physical libration around the synchronous state is commensurably with the mean-motion of the planet. Figure 3(a) shows the 2:1 secondary resonances.

Figure 3(c) shows that setting $e = 0.01$, both, the chaotic layer around the separatrix of the 1:1 resonance, and the domain of 2:1 secondary resonance, have large domains in the phase space. An orbit close to the 2:1 secondary resonance is shown in Figure 4(b). Note that, while the true anomaly and the rotation angle evolve at approximate same rate (period=0.34 days), the angle $\psi = f - \theta$ associated to the 1:1 resonance librates with twice of the period of motion.

The dynamics of rotation of KOI-55b is very similar to the case discussed above.

⁹ Note that ω_0 is a linear function of n with linear coefficient depending on the prolateness and $H(p, e)$. In the case of 1:1 resonance, at *first order* in eccentricity the relation between ω_0 and n is invariant to the value of eccentricity since $H(1, e) = 1$. This does not occur for large eccentricity for other low-order resonances like the 3:2 one, where $H(3/2, e) = \frac{7}{2}e$ at first order.

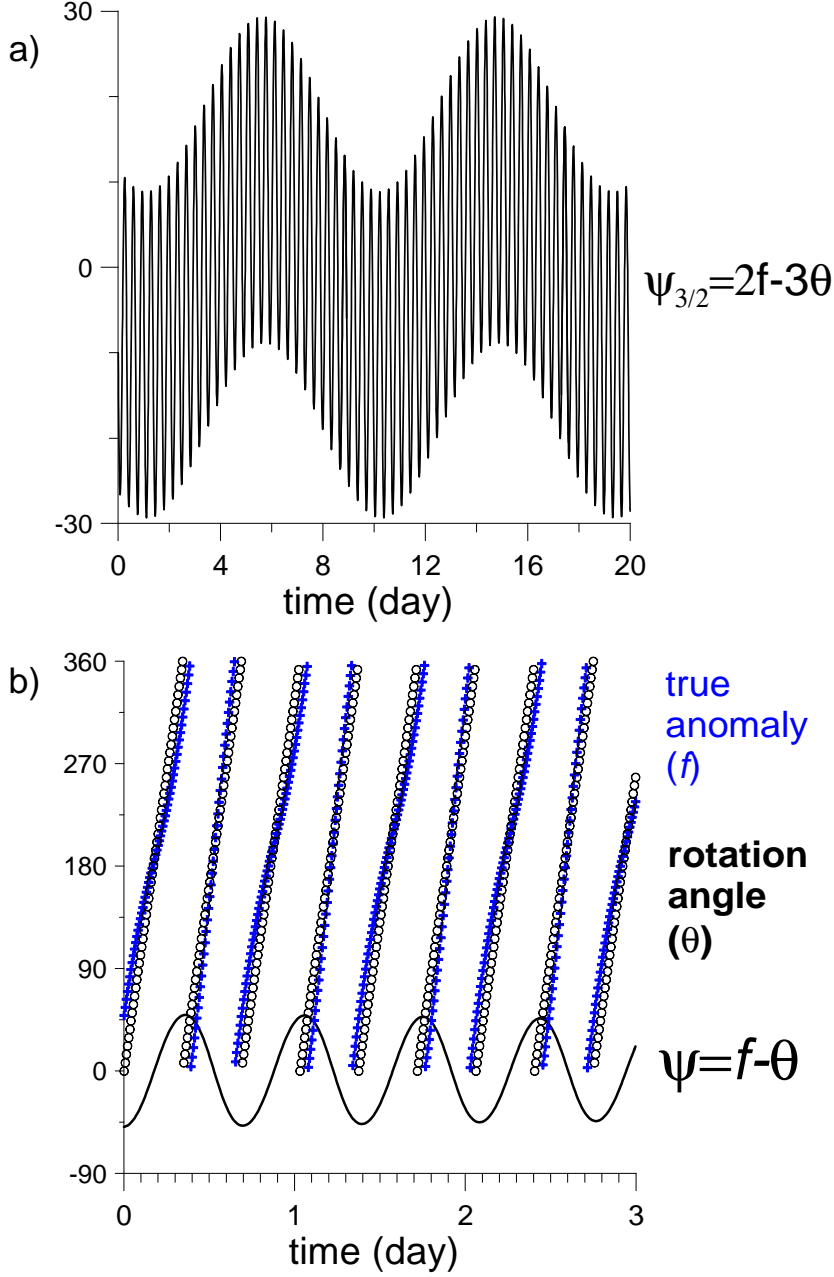


Fig. 4 (a) Time evolution of $\psi_{3/2} = 2f - 3\theta$. The initial condition corresponds to the small island within the 3:2 resonance indicated in Figure 3(b): $\theta_0 = 5^\circ$, $\dot{\theta}_0 = 1.685n$, $f_0 = 0^\circ$, where n is the mean motion. The long-term oscillation is the free libration while the short-term libration includes the forced one (see also Section 3.1.1). (b) Time evolution of different quantities indicated in the figure. The initial condition corresponds to the larger island of secondary resonance shown in Figure 3(c): $\theta_0 = 49^\circ$, $\dot{\theta}_0 = n$, $f_0 = 0^\circ$.

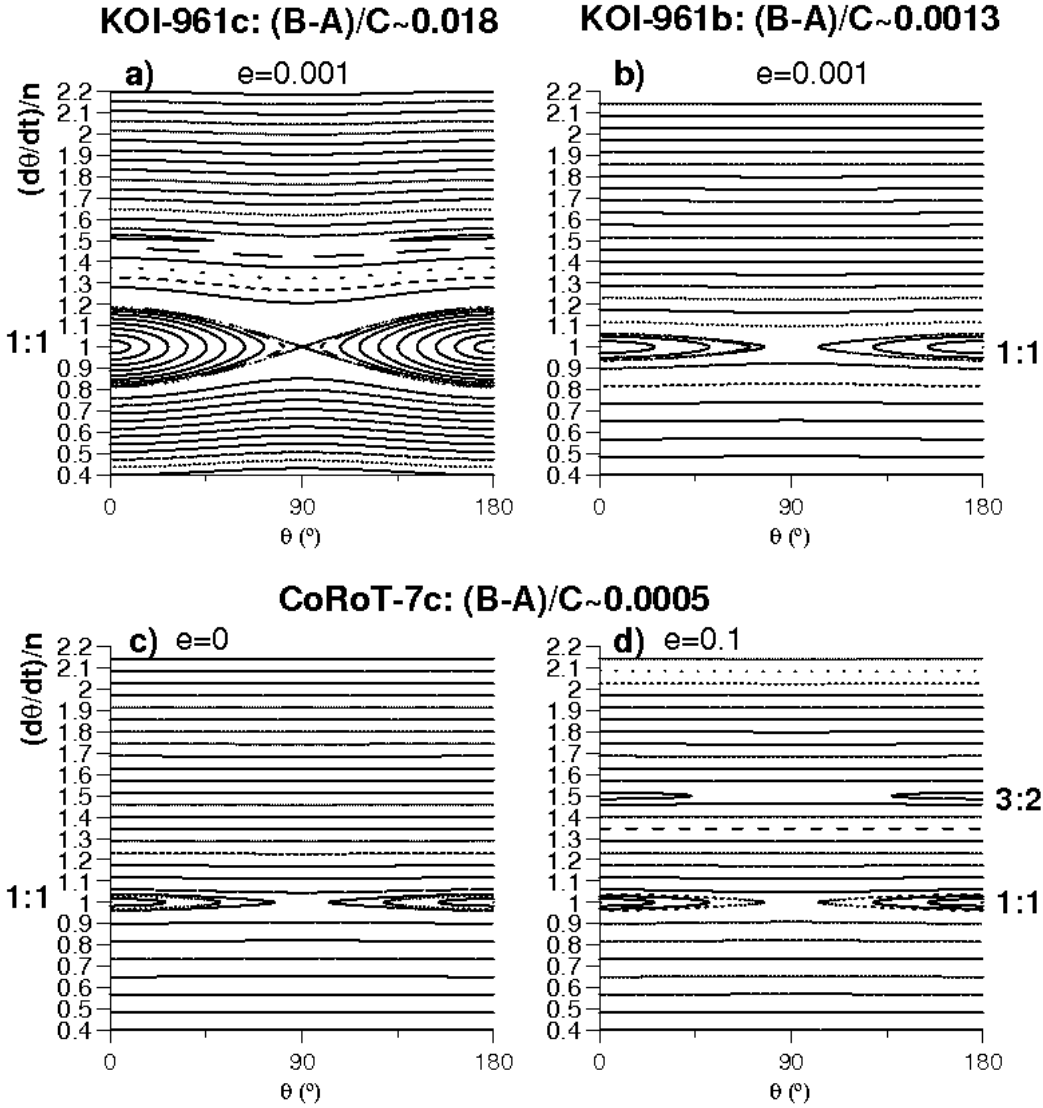


Fig. 5 Surfaces of Section in the plane $(\dot{\theta}/n \times \theta)$ of numerical solutions of (1). The sections have been done at each orbital revolution of the planets KOI-961c (a), KOI-961b (b), CoRoT-7c (c,d). Each orbit has been integrated for 1140 orbital periods of the planet. In (c,d), the numerical values of $\frac{B-A}{C}$ has been calculated with Equation (3) supposing that CoRoT-7c has the same radius of CoRoT-7b. Different values of the eccentricity have been used in the case of CoRoT-7c.

3.1.3 The system of KOI-961

The star KOI-961 hosts three transiting sub-Earth-sized planets (Muirhead et al. 2012). We estimate the $\frac{B-A}{C}$ of these planets (Table II). KOI-961c has the larger $\epsilon \sim 0.018$; its dynamics of rotation (Figure 5(a)) is very similar to the previous cases (e.g. Figure 2). The other two planets have relatively small values of $\epsilon \ll 0.01$ and the domain of the 1:1 resonance is very thin in their rotation phase space, like Figure 5(b) illustrates.

3.1.4 CoRoT-7c and the planets of the stars Kepler-18, 20 and 21

Earth-like candidate planets in *circular* orbits close to the star with semi-major axes larger than the previous cases have regular dynamics of rotation since their prolateness are small and the torque of star is negligible. The domain of the phase space of the synchronous resonance is very thin, like we show in Figure 5(c) in the case of CoRoT-7c, where we have supposed that its radius is equal to the radius of CoRoT-7b in order to estimate $\frac{B-A}{C} \sim \epsilon = 0.0005$.

In Figure 5(d) we put a fictitious value of orbital eccentricity of CoRoT-7c equal 0.1. A characteristic of the phase space in these cases is that the domains of the 3:2 and 1:1 resonance have similar width in the phase space.

Supposing circular orbit, analyses similar to that given in Figure 5(c) hold to Kepler-21b, Kepler-18b and Kepler-20b, close-in planets with orbital parameters with same order of magnitude of CoRoT-7c's (see Table I). However, Kepler-21b, Kepler-18b and Kepler-20b are transiting planets and we can give an estimative of their values of $\frac{B-A}{C}$, which are listed in Table II. Table II include also the $\frac{B-A}{C}$ of Kepler-20e and Kepler-20f, two planets present in the Kepler-20 system which have masses and orbital periods whose values are given within the range considered in this work (see Table I).

3.1.5 Planetary System of Kepler-11

The value of ϵ for the close-in planets of the star Kepler-11 are listed in Table II. Their values are small and the dynamics of rotation the planets are regular in our model.

3.2 Planets with eccentric orbits with $P < 7.5$ days present in multi-planetary systems

3.2.1 GJ 876d and Kepler-9d

Kepler-9d and GJ 876d are probably are small planets belonging to multiple systems where the outer members are hot Jupiters and whose orbits are close to the 2/1 mean-motion resonances. GJ 876d and Kepler-9d are two planets with similar orbital period and mass. They orbit around stars with very different values of mass since GJ 876 is a M4 V star with mass $\sim 0.334M_{SUN}$ (Correia et al. 2010), while Kepler-9 is a solar-type star with mass $m_0 \sim 1M_{SUN}$ (Torres et al. 2011). Kepler-9d is a planet whose radius is determined but the orbital eccentricity is not. On the other hand the eccentricity of GJ 876d is known (while its radius is not). Therefore we consider the value of ϵ as a free parameter in the case of Gliese 876d, and the orbital eccentricity in the case of Kepler-9d.

If GJ 876d is a terrestrial-like, solid planet, Valencia et al. (2007b) show that its radius cannot be larger than $\sim 12,000 \text{ km} \simeq 1.88R_E$. Adopting this value of radius we estimate the prolateness of this planet: $\frac{B-A}{C} \sim 0.0036$. GJ 876d has one of the largest reported orbital eccentricities among all the close-in Earth-like candidates. In order to study its rotation with our model we use the values of the eccentricity given in Correia et al. (2010), $e = 0.124$, and the value $e = 0.207$ given in Rivera et al. (2010). The results are shown in Figures 6(a,b). Within the above scenario we see by inspection of the surfaces of section that the rotation of Gliese 876d is probably regular within the domain of our model. It is interesting to note in this figure that the domains of 2:1 and 3:2 resonances have similar widths in the phase space.

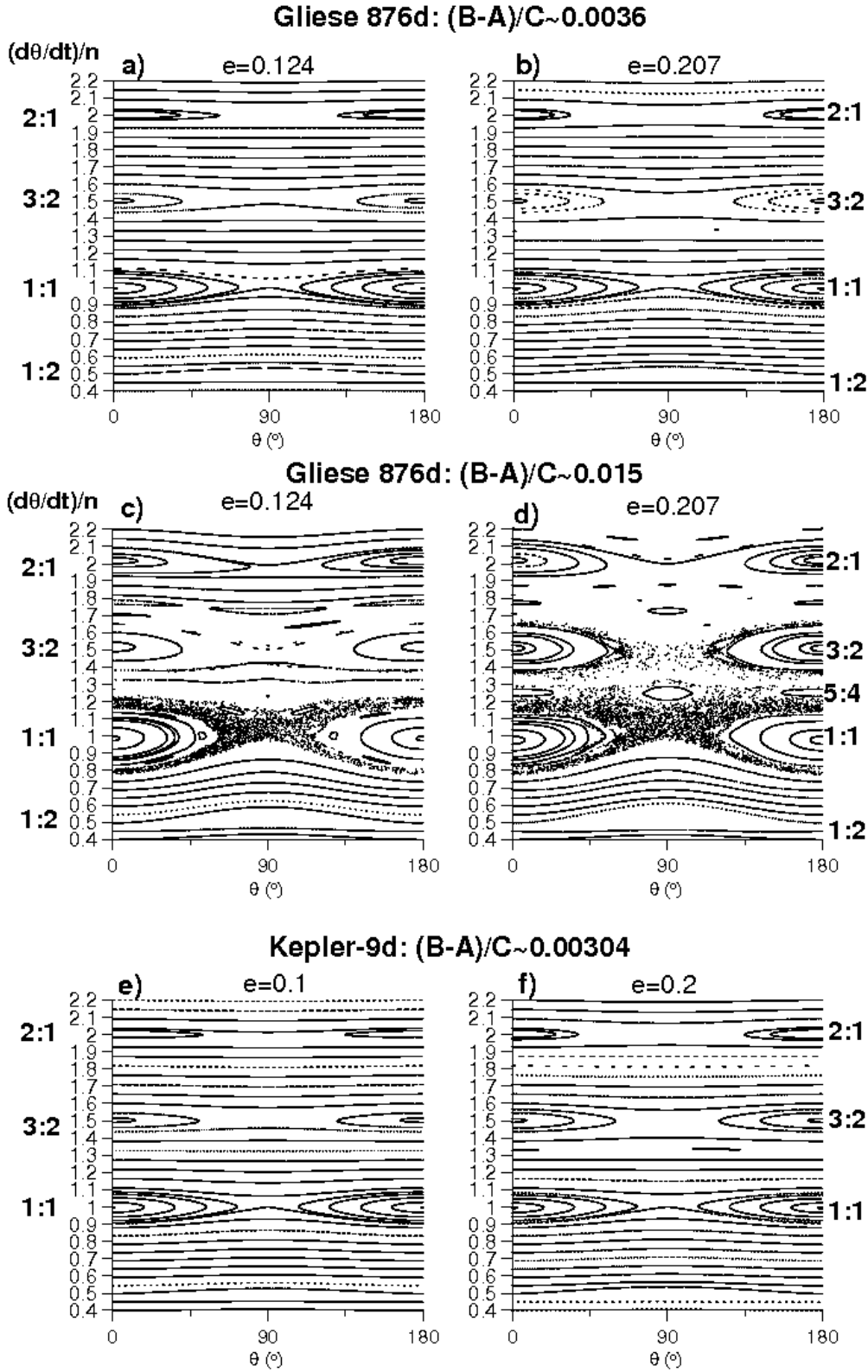


Fig. 6 Surfaces of Section in the plane $(\dot{\theta}/n \times \theta)$ of numerical solutions of (1). The sections have been done at each orbital revolution of the planet Gliese 876d (figures (a-d)) and Kepler-9d (e,f). Each orbit has been integrated for 1140 orbital periods of the planet. $\frac{B-A}{C}$ of Kepler-9d is given in Table II; in the case of Gliese 876 d the value of $\frac{B-A}{C}$ is discussed in Section 3.2.1. In (a,b) the orbital eccentricities correspond to two published values (see references in Section 3.2.1), while in (c,d) the eccentricities utilized in the simulations are fictitious.

The radius of GJ 876d is unknown, so we also study its dynamics with a larger value than that given above: $R \sim 3R_E \simeq 19,000$ km. From the plots similar to those shown in Figure 1 (Section 2), we can see that for this radius $\epsilon \sim 0.01$. Figures 6(c,d) show that the rotation can be more complicated in this case. For instance, we can see the overlap of the separatrix of the 3:2 and 1:1 resonances, engulfing the 5:4 resonance, when $e = 0.207$ (Figure 6(d)). All resonances, including the island of 1:2 resonance, have larger and similar domains in the phase space in the case of large ϵ (compare Figures 9(a,b) and Figure 6(c,d)).

The eccentricity of Kepler-9d is unknown, but in analogy to the case of GJ 876d, we study the dynamics of its rotation in the case of eccentric orbit. We investigate the dynamics of Kepler-9d for two values of eccentricity: $e = 0.1$ (Figure 6(e)) and $e = 0.2$ (Figure 6(f)). The rotation of Kepler-9d is regular in both cases.

The similarities between Figures 6(a,b) and Figures 6(e,f) are evident. The value of ϵ estimated for Kepler-9d and GJ 876d which have been utilized in these figures are similar: $\epsilon \sim 0.003$; we recall that the ϵ of GJ 876d was calculated supposing $R \simeq 1.88R_E$ given in the theory of Valencia et al. (2007b). Adopting the mass-radius relation of Valencia et al. (2007a), Kepler-9d is probably a solid-like body and our results on its dynamics of rotation are confident in this case. The case where we consider $\epsilon = 0.015$ for GJ 876d must be understood as a first view of a more complicated scenario since in this case the planet is not a solid-like body (Valencia 2007b).

3.2.2 55 Cnc e

55 Cnc e is a low-mass planet which has the smaller orbital period among all planets orbiting a solar-like star (G8-K0). With the recent estimative of its radius, it is probably that this body is an Earth-like planet with important rock-component in its structure (e.g. Gillon et al. 2012)¹⁰, a result which motivate us to study some aspects of its rotation with our model.

55 Cnc e has the second larger value of ϵ which we have calculated for all Super-Earths considered in this work (Table II). Figure 7 shows four plots for this planet where we adopt different values for the orbital eccentricity. The dynamics of rotation is essentially regular in the immediate vicinity of the resonances for $e < 0.01$. For larger values, like the case corresponding to the larger published value of the eccentricity ($e = 0.057$), is shown in Figure 7(c). In this case there is a large chaotic region around the separatrix of the 1:1 resonance. For larger values of eccentricity, a large region of chaos located between the 1:1 and 3:2 appears in the phase space (Figure 7(d)). Note also the presence of 1:4 secondary resonance inside the synchronous island¹¹.

In order to confirm and to explore in more details the properties of the phase space given by the surfaces of section we compute, in Figure 7(e), a dynamical map in a grid of initial conditions corresponding to range of the axis given in Figure 7(c). In the dynamical maps we plot the spectral number, N , defined by the number of peaks given in the numerical Fourier spectrum of some variable of the problem which are greater than a fraction of the highest amplitude (e.g. Callegari and Yokoyama 2012). We adopt reference amplitude of 10% of the largest peak present in the spectrum of θ . N is represented on each point of the grid by a color given in a gray scale which value depends of N in the following way: i) white points corresponding to $N = 1$; ii) gray points where $1 < N < N_c$, with N_c being a (arbitrarily) large value adopted for N ; iii) black points with $N \geq N_c$. We adopt $N_c = 100$ in Figure 7(e). Distinct regions are different stability regions of the phase space: in white and gray regions the motion is regular, where the spectra of the solutions contains a small number of separated and countable peaks. In darker regions, where the spectrum contains a large number of peaks, the motion can be chaotic, and in general the peaks are not well separated in the spectrum. Comparison and inspection of Figures 7(c,e) show us that the dynamical map of frequencies

¹⁰ According to Valencia (2007a), supposing a solid-like structure for 55 Cnc e, its radius cannot be larger than $\simeq 1.8R_E$. Since the estimated radius of 55 Cnc e is $\simeq 2.17R_E$ it cannot be considered a pure solid-like planet, admitting a non-negligible layer of other components like water in its composition. Thus, it can be interesting to improve our model to consider the perturbations in the rotation of planet adopting different layers (e.g. van Hoolst et al. 2008).

¹¹ Wisdom (2004) shows that, in the case of regular satellites of the Solar System, a capture in such rotational state may enhance the tidal heating in the satellite interior by several orders of magnitude. The same would occur for close-in Super-Earths.

agrees very well with the main dynamical regions of the system obtained with the surfaces of section (i.e., spin-orbit resonances, chaotic layers, secondary resonances).

We conclude that a non-null value of the eccentricity of 55 Cnc e, and its proximity to the star, lead a strong periodic perturbation on its rotation. Thus, according to our model, in a evolutionary scenario where some dissipative mechanism is able to reduce the primordial spin of the planet to the synchronous resonance, 55 Cnc e would have crossed a chaotic layer before the synchronism be attained, similar to the history of the rotation dynamics of the irregularly shaped, close-in, satellites of the solar system (Wisdom et al. 1984, Wisdom 1987, Wisdom 2004). This conjecture has been confirmed by Rodríguez et al. (2012) in their scenario of tidal evolution of the system of 55 Cnc.

3.3 Systems with a single planet

We consider in this separated section some aspects of the dynamics of rotation of systems with a single planet. Consider the cases of planets with circular and eccentric orbits separately.

The systems with single planets in *circular* orbit which we study are: HD 156668b (orbital period $P = 4.646\text{days}$, $m = 4.16M_E$), GJ 176b ($P = 8.78\text{days}$, $m = 8.42M_E$) and HD 125595b ($P = 9.67\text{days}$, $m = 14.3M_E$). The radius of all of them are unknown quantities, but we can use Figures 4(g,h,i,k) to infer that their prolateness are negligible due to their relatively large mass and planet-star distance ($a > 0.05\text{AU}$). Therefore their rotations suffer very small perturbation of their respective stars. In the case of HD 156668b the prolateness is slightly larger than the other cases due to its relatively smaller mass and distance to the star, but anyway its rotation is regular since we assume circular orbits.

There are several examples of isolated Super-Earths with reported *eccentric* orbits: GJ 3634b ($P = 2.64\text{days}$, $e = 0.08$, $m = 7.0M_E$), GJ 674b ($P = 4.7\text{days}$, $e = 0.1$, $m = 11.76M_E$), HD 7924b ($P = 5.4\text{days}$, $e = 0.17$, $m = 9.27M_E$), HD 45184b ($P = 5.88\text{days}$, $e = 0.3$, $m = 12.7M_E$), HD 97658b ($P = 9.5\text{days}$, $e = 0.17$, $m = 8.3M_E$). Except in the case of GJ 3634b, we can note that their masses are large and their radius would also be large in the scenario of solid-like planet given in Valencia et al. (2007a). However in all cases the prolateness are $\epsilon \ll 0.01$ and dynamics of rotation is regular, like several other cases shown previously, in spite of their eccentric orbit.

The case of GJ 3634b is different due to its proximity to GJ 3634 and relatively small mass. In this case, due to the similarities of the values of the parameters of the star-planet system with the system GJ 876d, we can use the results of the Section 3.2.1 to infer that the dynamics of rotation of is regular in spite of a probably non-negligible value of prolateness.

3.4 Other cases: GJ 1214b and GJ 581g

GJ 1214b has a mass within the interval $m < 10M_E$, but as shown in Charbonneau et al. (2009) and Valencia (2011), due its large radius, it may have a substantial gas layer and cannot be considered a solid-like planet. Our model is not adequate to this kind of structure but we speculate on the dynamics of rotation of GJ 1214b on basis of our model. And we also use this planet to give an application of the Chirikov's overlap criterium.

Figure 8 shows four plots where we consider our estimative value of $\epsilon = 0.0186$ (Table II). Four values of eccentricity, beginning with $e = 0.27$ (the maximum admitted value by Charbonneau et al. 2009), has been used to compute the sections. The results showed in Figure 8(a) shows a large region of chaotic motion close to the main resonances¹². For smaller values of eccentricity, the chaotic regions are confined close to the separatrices (e.g. Figure 8(b)).

¹² Our numerical experiments show that in the cases of strong perturbation, the domain of the 1:2 resonance is preserved from the chaotic regions located close to it. Wisdom (1984), in their study on the rotation of the satellite Hyperion, discuss this property of the 1:2 resonance. In fact, analyses of the averaged torques associated to the 1:1 and 1:2 spin-orbit resonances show that they are the strongest ones among all low-order resonances (e.g. Goldreich and Peale 1966).

55 Cnc e: $(B-A)/C \sim 0.028$

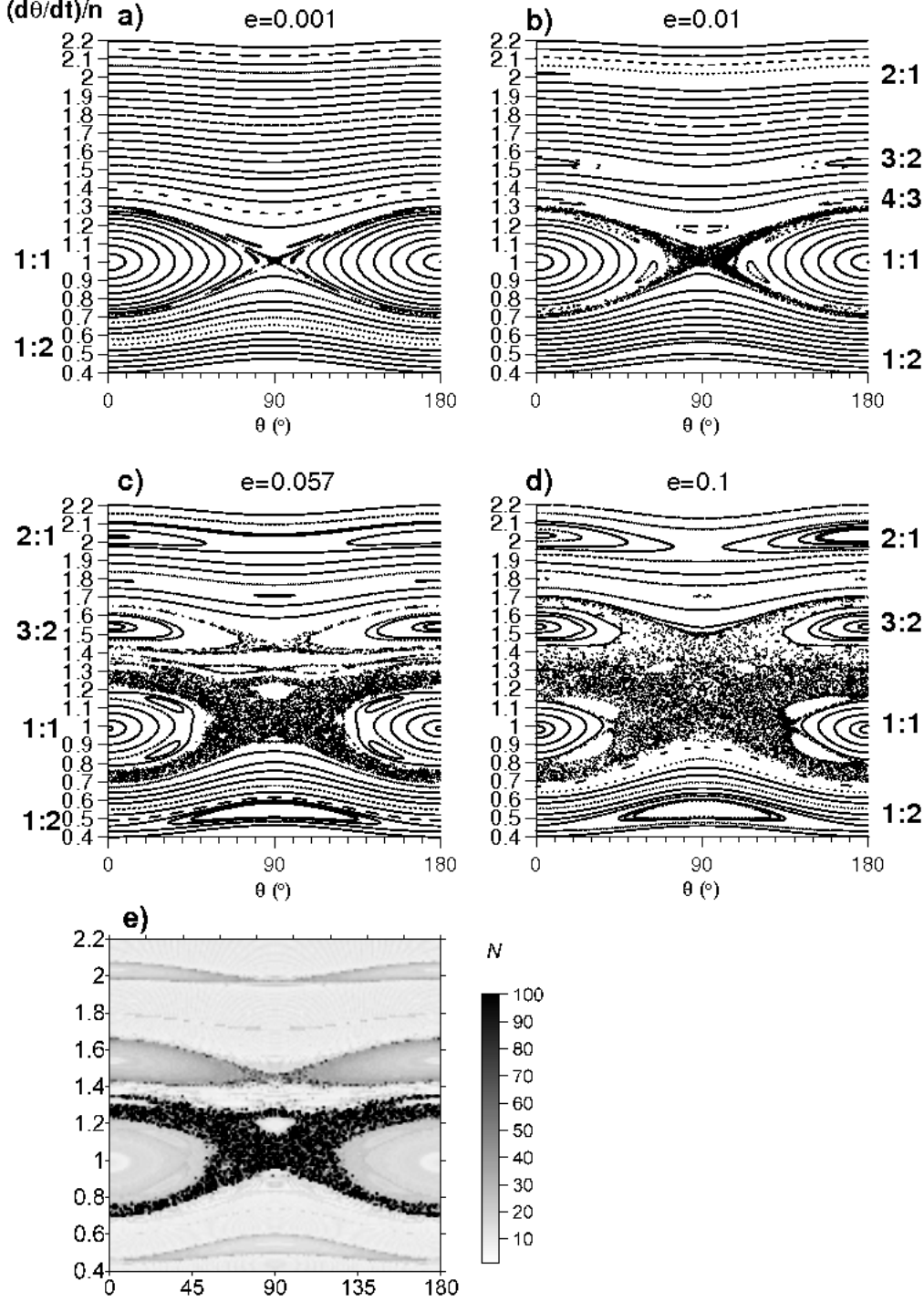


Fig. 7 Surfaces of Section in the plane $(\dot{\theta}/n \times \theta)$ of numerical solutions of (1). The sections have been done at each orbital revolution of the planet 55 Cancr e adopting different values of the orbital eccentricity which are indicated at the top of the plots. Each orbit has been integrated for 1140 orbital periods of the planet. The current (published) value of eccentricity is considered in (c) while the other values are fictitious. $\frac{B-A}{C} \sim \epsilon = 0.028$ are estimated adopting $R = 2.17R_E$ for the radius of the planet. (e) Dynamical map (see Section 3.2.2) in a grid of 22,801 points corresponding to (c).

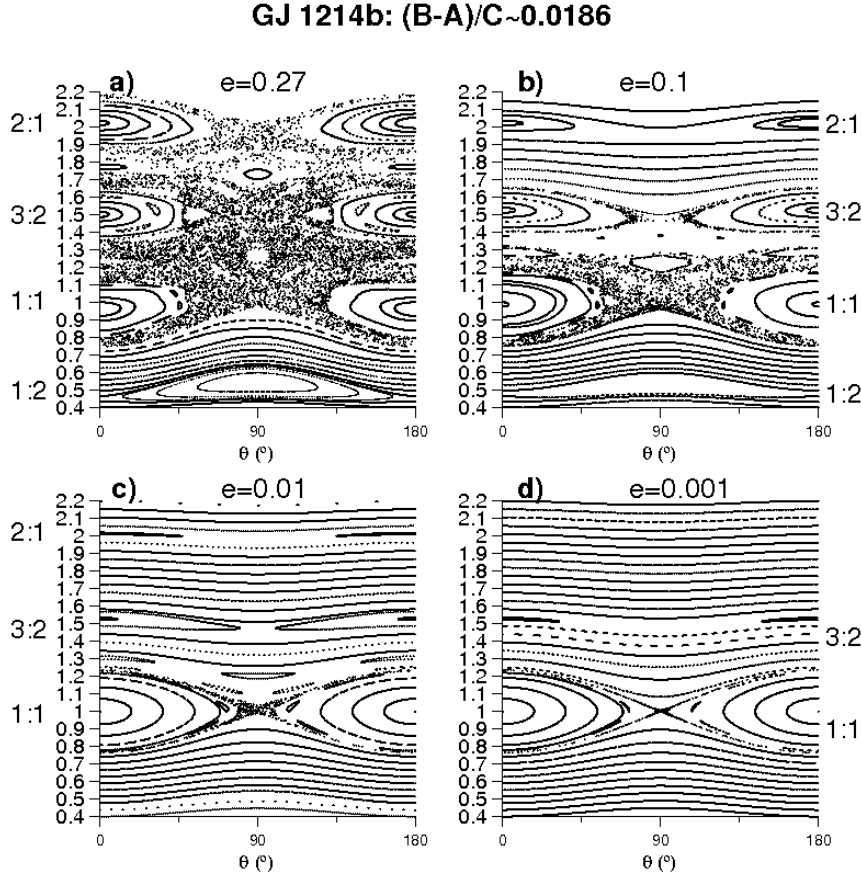


Fig. 8 Surfaces of Section in the plane $(\dot{\theta}/n \times \theta)$ of numerical solutions of (1). The sections have been done at each orbital revolution of the planet GJ 1214b, for four different values of the orbital eccentricity within the interval $e < 0.27$ (Charbonneau et al. 2009). Each orbit has been integrated for 1140 orbital periods of the planet.

The other plots given in Figures 8(c,d) correspond to smaller values of the eccentricity and show that the dynamics is regular and the domain of the 1:1 resonance is the largest one in the phase space.

We can use the Chirikov's overlap criterium to estimate local chaos around the main resonances in terms of the main parameters of the problem: $\frac{B-A}{C}$ and eccentricity. In fact, the separatrices of 1:1 and 3:2 resonances overlap for all values of $\frac{B-A}{C}$ larger than a critical quantity which is given by the following expression:

$$\left(\frac{B-A}{C}\right)_{critical} \sim \frac{1}{3} \left(\frac{1}{2 + \sqrt{14e}}\right)^2. \quad (7)$$

(Wisdom et al. 1984).

Figure 9 shows the plot of the critical $\left(\frac{B-A}{C}\right)_{critical}$ as a function of eccentricity. For $e = 0.27$, the critical value is 0.022. We can see that this value is very close to $\epsilon = 0.0186$, which has been calculated for GJ 1214b. Thus, in this case the overlap occurs, what is in well agreement with the result obtained in the surfaces of section (Figure 8(a)). For smaller values of eccentricity ($e = 0.1$ for instance), $\frac{B-A}{C}$ would be larger than 0.0186 for overlap to occur

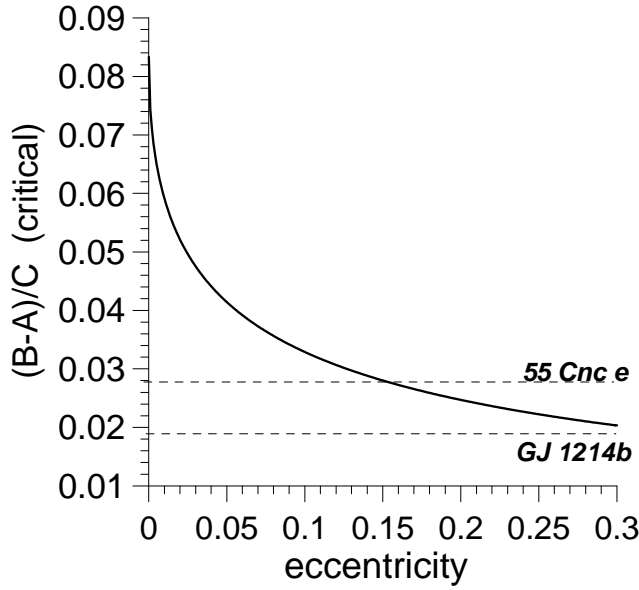


Fig. 9 Critical values of $\frac{B-A}{C}$ for overlap of the 1:1 and 3:2 spin-orbit resonances calculated from Equation (7), Section 3.5. The horizontal dashed lines indicate the values of $\frac{B-A}{C}$ of the planets indicated in the figure.

according to the Equation 7, and for this reason the overlap of the 1:1 and 3:2 resonances does not occur in the surface of section (Figures 8(b)).

We can make an analysis similar to this given above for all other cases shown in this paper. For instance, in Figure 9 we indicate the value of $\epsilon = 0.028$ calculated for 55 Cnc e, and we have that, for $e = 0.15$ the overlap occurs. Figures 9(c,d) show good agreement between the surfaces of section and the Chirikov's overlap criterium: for $e < 0.1$ the separatrices of the 1:1 and 3:2 do not overlap (Figures 7(b,c)) but for $e = 0.1$ (Figure 7(d)), a valor very close to the critical one, the overlap occurs.

Figure 9 shows that for large values of $\frac{B-A}{C} \sim 10^{-1}$ the overlap may occur for very small value of eccentricity $\sim < 0.01$. This is shown in Figure 3(c) in the case of KOI-55c.

GJ 581 g

We give here some comments about the dynamics of rotation of GJ 581 g. This planet, although not yet surely confirmed (see Tadeu dos Santos et al. 2012), would have a very small $m \sim 3.1M_E$, which would imply in a relatively large value of ϵ . However, due to its relatively large distance from GJ 581 ($r \sim 0.14$ AU), and the slow-mass star, its prolateness is negligible, and its rotation is regular within the domain of our model.

4 Conclusions and Discussion

We have explored the dynamics of rotation of close-in exoplanets with a model often applied in studies of physical libration of natural satellites and Mercury (Goldreich and Peale 1966, Henrard 1985, Bills et al. 2009). This model is suitable to quantify the main effects of the gravitational torque of the star on the rotation of the planet when the obliquity of the axis of rotation of planet is considered fixed (i.e., we neglect the motion in attitude).

The model is valid in the hypothesis of a rigid planet and therefore we neglect in our calculations the effects of tidal torques of the central star on the rotation of the planet. Thus, we

study the conservative dynamics of rotation of several possible Earth-like exoplanets. This type of planet, which mass is $m < 10M_E$, may admit a permanent solid structure depending also on the value of the radius of the planet (e.g. Valencia et al. 2007a, 2011). Our methodology was based in previous works like Wisdom et al. (1984, 1987, 2004), where the dynamics of rotation of regular satellites of Saturn and Phobos and Deimos are numerically explored through analysis of surfaces of section.

According to the *conservative model*, the effects of the torque of the star on the rotation of the planet depends basically on two parameters: the eccentricity of the orbit, and the existence of a permanent equatorial bulge (the prolateness, ϵ) of an ellipsoid with semi-axes $a > b > c$. A non-null value of the prolateness implies that $\frac{B-A}{C} \neq 0$, where A, B, C are the main moments of inertia which, in the case of exoplanets, are completely unknown quantities. We show in this work that $\frac{B-A}{C} = \epsilon$, a relation valid at first order in ϵ when $b = c$. On the other hand ϵ can be written as function of the masses of the system, the star-planet distance and the radius of the planet, and when these parameters are known, we can estimate an order of magnitude of ϵ . In general the transiting planets have a determination of the radius. When the planet is not a transiting one we show here how to obtain a significant range of the planet prolateness in terms of the several parameters of the star-planet system.

We discuss the cases of Super-Earths candidates immersed in multi-planetary systems and those which are single planets. We also consider planets in circular and eccentric orbits. In the case of *circular* orbits the dynamics of rotation of exoplanets is trivial, i.e., it is regular and the synchronous state governs the phase space with a domain dictated only by the magnitude of the prolateness of the equator and the mass of the central star. The most interesting cases are close-in exoplanets with eccentric orbits, since in this case the dynamics of physical libration may deviate significantly from the pendulum analogy. Large-scale chaotic motion of rotation for initial conditions close to the separatrix of the main resonances appears due to a combination of large prolateness and high eccentricity.

Our main results on the dynamics of rotation of some cases studied here are summarized below:

- KOI-55b,c, close-in planets with very small mass ($m < 1M_E$) have large prolateness $0.1 < \epsilon < 0.2$ and, even for small eccentricity ($e \sim 0.007$), the separatrices of the 1:1 and 3:2 resonance overlap leading to the possibility of complicated dynamics of rotation of the planet around the synchronous motion.
- The rotation of planets like Kepler-10b CoRoT-7b, KOI-961c can suffer strong effects of the star due to their relatively large values of their prolateness, which are given in the interval: $0.01 < \epsilon < 0.02$. However, their orbits are probably circular and the phase spaces of rotation are dominated by the circulatory regimes and libration around the synchronous island, which domain is large and is probably the loci of the current state of the rotations of this kind of planet.
- Planets with prolateness $\epsilon \ll 0.01$ and quasi-circular orbits have the phase space dominated by circulation regimes of motion, and the width of the synchronous resonance is very small in the phase space. As examples we can cite CoRoT-7c and KOI-961b.
- Close-in planets in *eccentric* orbits and orbital period $P < 7.5$ days admit complicated dynamics depending on the value of the radius (R) and the mass (m). In fact, the larger is R , the larger is the prolateness; the larger is the m , the smaller is the prolateness. For instance, GJ 876d can have large prolateness $\epsilon > 0.01$ if $R \sim 3R_E$. It is improbable that 61 Vir b has non-negligible prolateness in the case of $R \gg 3R_E$. Kepler-9d, Gl 581e, HD 215487b have small prolateness $\epsilon \ll 0.01$ and the rotation phase spaces are regular. For eccentricities larger than 0.1, we have observed that in some cases (e.g. HD 215487b, Kepler-9d) the domains of the 3:2 and 1:1 resonances have very similar widths in the phase space.
- 55 Cnc-e admits a large chaotic regions close the synchronous rotation adopting its current parameters ($e = 0.057$, $m \sim 8.58M_E$, $R = 2.17R_E$, $\epsilon \sim 0.028$). The implications of the chaos on the evolution through spin-orbit resonance are being investigated in another work (Rodríguez et al. 2012).

All simulations show that the dynamics of rotation of close-in *eccentric* Earth-like planets may have a complex behavior close to the regions of separatrices in the phase space depending on the prolateness. In a scenario including the action of a dissipative force which acts to spin down the primordial rotation, one should understand how planetary rotation of all bodies studied here evolves to synchronism traversing a chaotic region of the phase space (e.g. Rodríguez

et al. 2012)¹³. Even in those cases with almost circular orbits, the rotation can be driven to a complex motion when $\frac{B-A}{C}$ is large (e.g. KOI-55b,c).

- The dynamics of planets with *eccentric orbits* and ($P > 7.5$ days) have also been studied here (e.g. Gl 581c, HD 181433b, HD 215487c). We have shown that all of them have negligible prolateness in the case we suppose a solid structure for them. Therefore they probably have regular motion of rotation around the synchronous or other main spin-orbit resonances.

- The prolateness of several single Earth-like candidates planets considered here (e.g. GJ 176b, GJ 674b, HD 97658b) may be negligible due to both their large values of mass and distance from the star. Therefore their dynamics of rotation are regular in spite of eccentric orbits (GJ 674b, HD 97658b). On the other hand the planet GJ 3634b has probably a non-negligible prolateness $\epsilon \sim 10^{-3}$. With this value as reference, Rodríguez et al. (2012) show simulations where this planet may be currently captured into the 2:1 spin-orbit resonance.

Discussion on Tidal Evolution

- Due to tidal effects it is expected that the orbit of a close-in planet be circular. In Appendix A we calculate the timescale for circularization of a planet with elements similar to CoRoT-7b. We confirm previous results which show that state that planets with orbital period $P > 8$ days may admit a non-circular orbit since the time scale for circularization is very large: > 10 billion years. Since the value of orbital eccentricity of some planets are still being improved (see Tadeu dos Santos et al. 2012) we consider in our calculations several values of eccentricity in addition to the ones given in literature.

- We can also apply our calculations given in Appendix A for several single planets discussed in Section 3.4. The orbital periods of GJ 3634b, GJ 674b, HD 7924b and HD 45184b are smaller than 6 days and thus it is expected a circular orbit in view of the tidal effect. On the other hand, it is not be expected a null eccentricity for HD 125595b since $P \sim 9.4$ days.

- Although we have neglected the effects of tidal torques in this work, they would be important in the case of a non-rigid planet located very close to the central star. In Appendix B we study the case of the planet CoRoT-7b utilizing a model of tides where the phase lags depend linearly with the corresponding tidal frequency. We calculate the magnitude of the tidal torque and compare with the gravitational torque due to the equatorial prolateness in order to evaluate the stability of two spin-orbit resonances, the synchronous and 3:2 spin-orbit resonances. The 1:1 resonance is stable adopting our estimative of $\epsilon = 0.0092$ for CoRoT-7b. The reader is referred to Rodríguez et al. (2012) for a detailed study of the coupled spin-orbit evolution of short-period rocky planets.

Acknowledgements FAPESP (2006/58000-2 (NCJ); 2009/16900-5 (ARC).)

References

1. Anglada-Escudé, G.; Lpez-Morales, M.; Chambers, John E.. How Eccentric Orbital Solutions Can Hide Planetary Systems in 2:1 Resonant Orbits. *The Astrophysical Journal*, **709**, 168-178 (2010).
2. Baraffe, I.; Chabrier, G.; Barman, T.. The physical properties of extra-solar planets. *Reports on Progress in Physics*, **73**, 1, pp. 016901 (2010).
3. Barnes, Jason W.; Fortney, Jonathan J.. Measuring the Oblateness and Rotation of Transiting Extrasolar Giant Planets. *The Astrophysical Journal*, **588**, 545-556 (2003).
4. Batalha, Natalie M.; Borucki, William J.; Bryson, Stephen T.; Buchhave, Lars A.; Caldwell, Douglas A.; Christensen-Dalsgaard, Jrgen; Ciardi, David; Dunham, Edward W.; Fressin, Francois; Gautier, Thomas N., III; and 42 coauthors. Kepler's First Rocky Planet: Kepler-10b. *The Astrophysical Journal*, **729** (2011).

¹³ Moreover, the evolution through resonances in the case of strong perturbation can result in the chaotic tumbling of the rotation axis of the planets, similarly to the case of some Solar System's bodies (Wisdom et al. 1984; 1987).

5. Batygin, K.; Bodenheimer, P.; Laughlin, G.. Determination of the Interior Structure of Transiting Planets in Multiple-Planet Systems. *The Astrophysical Journal Letters*, **704**, L49-L53 (2009).
6. Beutler, G.. *Methods of Celestial Mechanics*, Vol. I (Springer, Berlin) (2005).
7. Bills, B. G.; Nimmo, F.; Karatekin, O.; van Hoolst, T.; Rambaux, N.; Levrard, B.; Laskar, J.. Rotational Dynamics of Europa. In: *Europa*, Edited by Robert T. Pappalardo, William B. McKinnon, Krishan K. Khurana; with the assistance of René Dotson with 85 collaborating authors. University of Arizona Press, Tucson. The University of Arizona space science series ISBN: 9780816528448, p.119 (2009).
8. Callegari Jr., N., Yokoyama, T.. Numerical exploration of resonant dynamics in the system of Saturnian inner Satellites. *Planetary and Space Science*, **58**, 1906-1921 (2010).
9. Carter, Joshua A.; Winn, Joshua N.. Empirical Constraints on the Oblateness of an Exoplanet. *The Astrophysical Journal*, **709**, 1219-1229 (2010).
10. Castan, T., Menou, K.. Atmospheres of Hot Super-Earths. *The Astrophysical Journal Letters*, **743**, Issue 2, article id. L36 (2011).
11. Celletti, A.; Voyatzis, G.. Regions of stability in rotational dynamics. *Celestial Mechanics and Dynamical Astronomy*, **107**, 101-113 (2010).
12. Charbonneau, David; Berta, Zachory K.; Irwin, Jonathan; Burke, Christopher J.; Nutzman, Philip; Buchhave, Lars A.; Lovis, Christophe; Bonfils, Xavier; Latham, David W.; Udry, Stphane; and 9 coauthors. A super-Earth transiting a nearby low-mass star. *Nature*, **462**, 891-894 (2009).
13. Charpinet, S.; Fontaine, G.; Brassard, P.; Green, E. M.; van Grootel, V.; Randall, S. K.; Silvotti, R.; Baran, A. S.; stensen, R. H.; Kawaler, S. D.; Telting, J. H.. A compact system of small planets around a former red-giant star. *Nature*, **480**, 496-499 (2011).
14. Correia, A. C. M., Levrard, B., Laskar, J.. On the equilibrium rotation of Earth-like extra-solar planets. *Astronomy and Astrophysics*, **488**, L63-L66 (2008).
15. Correia, A. C. M.; Couetdic, J.; Laskar, J.; Bonfils, X.; Mayor, M.; Bertaux, J.-L.; Bouchy, F.; Delfosse, X.; Forveille, T.; Lovis, C.; Pepe, F.; Perrier, C.; Queloz, D.; Udry, S. . The HARPS search for southern extra-solar planets. XIX. Characterization and dynamics of the GJ 876 planetary system. *Astronomy and Astrophysics*, **511**, id.A21 (2010).
16. Correia, Alexandre C. M.; Bou, Gwenal; Laskar, Jacques. Pumping the Eccentricity of Exoplanets by Tidal Effect. *The Astrophysical Journal Letters*, Volume 744, Issue 2, article id. L23 (2012).
17. Danby, J. M. A.. *Fundamentals of Celestial Mechanics*, 2nd edition. Willmann-Bell Richmond (1988).
18. Dobrovolskis, A. R.. Spin states and climates of eccentric exoplanets. *Icarus*, **192**, 1-23 (2007).
19. Dobrovolskis, A. R.. Insolation patterns on synchronous exoplanets with obliquity. *Icarus*, **2004**, 1-10 (2009).
20. Dobbs-Dixon, I, Lin, D. N. C., Mardling, R. A.. Spin-Orbit Evolution of Short-Period Planets. *The Astrophysical Journal*, **610**, 464-476 (2004).
21. Everhart, E.. An efficient integrator that uses Gauss-Radau spacings. In: *IAU Colloquium* **83**, 185-202 (1985).
22. Ferraz-Mello, S., Rodríguez, A., Hussmann, H.. Tidal friction in close-in satellites and exoplanets: The Darwin theory re-visited. *Celest. Mech. Dyn. Astr.*, **101**, 171-201 (2008).
23. Ferraz-Mello, S.; Tadeu dos Santos, M.; Beauge, C.; Michtchenko, T. A.; Rodríguez, A.. On planetary mass determination in the case of super-Earths orbiting active stars. The case of the CoRoT-7 system. *A&A*, 531A (2011).
24. Forveille, T.; X. Bonfils, X. Delfosse, R. Alonso, S. Udry, F. Bouchy, M. Gillon, C. Lovis, V. Neves, M. Mayor, F. Pepe, D. Queloz, N.C. Santos, D. Segransan, J.M. Almenara, H. Deeg, M. Rabus. The HARPS search for southern extra-solar planets XXXII. Only 4 planets in the Gl 581 system. arXiv:1109.2505.
25. Gillon, M.; Demory, B.-O.; Benneke, B.; Valencia, D.; Deming, D.; Seager, S.; Lovis, Ch.; Mayor, M.; Pepe, F.; Queloz, D.; Sgransan, D.; Udry, S.. *Astronomy & Astrophysics*, Volume 539, id.A28 eprint (2012).
26. Goldreich, P., Peale, S.. Spin-orbit coupling in the solar system. *The Astronomical Journal*, **71**, 425-437 (1966).
27. Henrard, J. Spin-Orbit Resonance and the Adiabatic Invariant. In: S. Ferraz-Mello and W. Sessin (eds), *Resonances in the Motion of the Planets, Satellites and Asteroids*, IAG/USP, Sao Paulo, 19-26 (1985).

28. Hébrard, G.; Ehrenreich, D.; Bouchy, F.; Delfosse, X.; Moutou, C.; Arnold, L.; Boisse, I.; Bonfils, X.; Daz, R. F.; Eggenberger, A.; Forveille, T.; Lagrange, A.-M.; Lovis, C.; Pepe, F.; Perrier, C.; Queloz, D.; Santerne, A.; Santos, N. C.; Sgransan, D.; Udry, S.; Vidal-Madjar, A.. The retrograde orbit of the HAT-P-6b exoplanet. *Astronomy & Astrophysics*, **527**, id. L11 (2011).
29. Iess L., Rappaport N. J., Jacobson R. A., et al.. *Science*, **327**, 1367 (2010).
30. Jackson, B., Greenberg, R., Barnes, R.. Tidal Evolution of Close-in Extrasolar Planets. *The Astrophysical Journal*, **678**, 1396-1406 (2008a).
31. Jackson, B., Barnes, R., Greenberg, R.. Tidal heating of terrestrial extrasolar planets and implications for their habitability. *Mon. Not. R. Astron. Soc.*, **391**, 237-245 (2008b).
32. Jackson, B., Greenberg, R., Barnes, R.. Tidal heating of Extrasolar Planets. *The Astrophysical Journal*, **681**, 1631-1638 (2008c).
33. Kitiashvili, I. N.; Alexander, G.. Rotational evolution of exoplanets under the action of gravitational and magnetic perturbations. *Celestial Mechanics and Dynamical Astronomy*, **100**, 121-140 (2008).
34. Kramm, U.; Nettelmann, N.; Redmer, R.; Stevenson, D. J.. On the degeneracy of the tidal Love number k_2 in multi-layer planetary models: application to Saturn and GJ436b. *arXiv:1101.0997* (2011).
35. Lammer, H.; Khodachenko, M. L.; Khodachenko, M. L., Herbert, I. M., Lichtenegger, I. M., Kulinov, Y. N.. Impact of Stellar Activity on the Evolution of Planetary Atmospheres and Habitability. In: *Extrasolar Planets: Formation, detection and Dynamics*. Dvorak, R. (Ed.) (2008).
36. Lammer, H.; Bredeft, J. H.; Coustenis, A.; Khodachenko, M. L.; Kaltenegger, L.; Grasset, O.; Prieur, D.; Raulin, F.; Ehrenfreund, P.; Yamauchi, M.; and 7 coauthors. What makes a planet habitable? *The Astronomy and Astrophysics Review*, **17**, 181-249 (2009).
37. Léger, A.; Rouan, D.; Schneider, J.; Barge, P.; Fridlund, M.; Samuel, B.; Ollivier, M.; Guenther, E.; Deleuil, M.; Deeg, H. J.; and 151 coauthors. Transiting exoplanets from the CoRoT space mission. VIII. CoRoT-7 b: the first super-Earth with measured radius. *Astronomy and Astrophysics*, **506**, 287-302 (2009).
38. Léger, A.; Grasset, O.; Fegley, B.; Codron, F.; Albareda, A. F.; Barge, P.; Barnes, R.; Cance, P.; Carpy, S.; Catalano, F.; Cavarroc, C.; Demangeon, O.; Ferraz-Mello, S.; Gabor, P.; Griemeier, J.-M.; Leibacher, J.; Libourel, G.; Maurin, A.-S.; Raymond, S. N.; Rouan, D.; Samuel, B.; Schaefer, L.; Schneider, J.; Schuller, P. A.; Selsis, F.; Sotin, C.. The extreme physical properties of the CoRoT-7b super-Earth. *Icarus*, **213**, 1-11. (2011).
39. Levrard, B., Correia, A. C. M., Chabrier, G., Baraffe, I., Selsis, F., Laskar, J.. Tidal dissipation within hot Jupiters: a new appraisal. *Astronomy and Astrophysics*, **462**, L5-L8 (2007).
40. Mardling, R. A.. Long-term tidal evolution of short-period planets with companions. *Monthly Notices of the Royal Astronomical Society*, Volume 382, Issue 4, pp. 1768-1790 (2007).
41. Matsumura, Soko; Takeda, Genya; Rasio, Frederic A. On the Origins of Eccentric Close-In Planets. *The Astrophysical Journal*, Volume 686, Issue 1, pp. L29-L32 (2008).
42. Michtchenko, T. A., Ferraz-Mello, S.. Resonant Structure of the outer solar system in the neighborhood of the planets. *The Astronomical Journal* **122**, 474-481 (2001).
43. Mignard, F.. The evolution of the lunar orbit revisited - I. Moon and Planets, **20**, 301-315 (1979).
44. Muirhead, Philip S.; Johnson, John Asher; Apps, Kevin; Carter, Joshua A.; Morton, Timothy D.; Fabrycky, Daniel C.; Pineda, John Sebastian; Bottom, Michael; Rojas-Ayala, Brbara; Schlawin, Everett; Hamren, Katherine; Covey, Kevin R.; Crepp, Justin R.; Stassun, Keivan G.; Pepper, Joshua; Hebb, Leslie; Kirby, Evan N.; Howard, Andrew W.; Isaacson, Howard T.; Marcy, Geoffrey W.; Levitan, David; Diaz-Santos, Tanio; Armus, Lee; Lloyd, James P.. Characterizing the cool kois. iii. KOI 961: a small star with large proper motion and three small planets. *The Astrophysical Journal*, Volume 747, Issue 2, article id. 144 (2012).
45. Murray, C. D., Dermott, S. F.. *Solar System Dynamics*, Cambridge University Press (1999).
46. Ragozzine, D.; Wolf, A. S.. Probing the Interiors of very Hot Jupiters Using Transit Light Curves. *The Astrophysical Journal*, **698**, 1778-1794 (2009).
47. Rivera, E. J., Gregory Laughlin, R. Paul Butler, Steven S. Vogt, Nader Haghighipour, Stefano Meschiari. The Lick-Carnegie exoplanet survey: a Uranus-mass fourth planet for GJ 876 in an extrasolar laplace configuration. *The Astrophysical Journal*, **719**, 890-899 (2010).
48. Rodríguez, A. C., Callegari, N. Jr., Michtchenko, T., Hussmann, H.. Spin-orbit evolution of hot Super-Earths. Pre-print. *Monthly Notices of the Royal Astronomical Society, MNRAS* (2012).

49. Rodríguez, A.; Ferraz-Mello, S.; Michtchenko, T. A.; Beaug, C.; Miloni, O.. Tidal decay and orbital circularization in close-in two-planet systems. *Monthly Notices of the Royal Astronomical Society*, 415, 2349-2358 (2011).
50. Rodríguez, A., Ferraz-Mello, S.. Tidal decay and circularization of the orbits of short-period planets. *EAS Publications Series*, **42**, 411-418 (2010).
51. Rodríguez, A.. *Evolução Orbital de Planetas Quentes Atribuída ao Efeito de Maré*. PhD Thesis, Universidade de Sao Paulo, Brazil, (2010).
52. Seager, S.; Hui, Lam. Constraining the Rotation Rate of Transiting Extrasolar Planets by Oblateness Measurements. *The Astrophysical Journal*, **574**, 1004-1010.
53. Showman, Adam P.; Polvani, L. M.. Equatorial Superrotation on Hot Jupiters. *The Astrophysical Journal*, **738**, Issue 1, article id. 71 (2011).
54. Schubert G., Anderson J. D., Spohn T., McKinnon W. B.. Jupiter. *The Planet, Satellites and Magnetosphere*, 281. (2004).
55. Spiegel, David S.; Raymond, Sean N.; Dressing, Courtney D.; Scharf, Caleb A.; Mitchell, Jonathan L.. Generalized Milankovitch Cycles and Long-Term Climatic Habitability. *The Astrophysical Journal*, **721**, 1308-1318 (2010).
56. Tadeu dos Santos, M. G. G. Silva S. Ferraz-Mello T.A. Michtchenko. A new analysis of the GJ581 extrasolar planetary system. *Celestial Mechanics and Dynamical Astronomy*, In press (2012).
57. Torres, Guillermo; Fressin, Francois; Batalha, Natalie M.; Borucki, William J.; Brown, Timothy M.; Bryson, Stephen T.; Buchhave, Lars A.; Charbonneau, David; Ciardi, David R.; Dunham, Edward W.; and 20 coauthors. Modeling Kepler Transit Light Curves as False Positives: Rejection of Blend Scenarios for Kepler-9, and Validation of Kepler-9 d, A Super-earth-size Planet in a Multiple System. *The Astrophysical Journal*, **727**, Issue 1, article id. 24 (2011).
58. van Hoolst, T.; Rambaux, N.; Karatekin, .; Dehant, V.; Rivoldini, A.. The librations, shape, and icy shell of Europa. *Icarus*, Volume 195, Issue 1, p. 386-399 (2008).
59. Valencia, Diana; Sasselov, Dimitar D.; O'Connell, Richard J.. Detailed Models of Super-Earths: How Well Can We Infer Bulk Properties?. *The Astrophysical Journal*, **665**, 1413-1420 (2007a).
60. Valencia, D., Sasselov, Dimitar D.; O'Connell, Richard J.. Radius and Structure Models of the First Super-Earth Planet. *The Astrophysical Journal*, **656**, 545-551 (2007b).
61. Valencia, D.. Characterising Super-Earths. *EPJ Web of Conferences*, **11**, 03001 (2011).
62. Zuluaga, Z. I., Cuartas, P. A.. The role of rotation on the evolution of dynamo generated magnetic fields in Super Earths. *Icarus* 217, 88-102 (2012).
63. Wisdom, J., Peale, S. J., Mignard, F.. The chaotic rotation of Hyperion. *Icarus*, **58**, 137-152 (1984).
64. Wisdom, J.. Rotational dynamics of irregularly shaped natural satellites. *The Astronomical Journal* **94**, 1350-1360 (1987).
65. Wisdom, J.. Spin-Orbit Secondary Resonance Dynamics of Enceladus. *The Astronomical Journal* **128**, 484-491 (2004).
66. Wisdom, J.. Tidal dissipation at arbitrary eccentricity and obliquity. *Icarus*, **193**, 637-640 (2008).

Appendix A: Orbital circularization due to tidal effect

We consider a slow-rotating star and a close-in planet interacting pair. The aim is to analyze the timescale for orbital circularization due to tidal interaction. We refer to Ferraz-Mello et al. (2008) and Rodríguez and Ferraz-Mello (2010) for assumptions, definitions of quantities and further details.

The averaged variation of the eccentricity due to the combined effects of stellar and planetary tides is given by

$$\langle \dot{e} \rangle = -\frac{1}{3} n e a^{-5} (18\hat{s} + 7\hat{p}), \quad (8)$$

where

$$\hat{s} = \frac{9}{4} \frac{k_{20}}{Q_0} \frac{m}{m_0} R_0^5 \quad ; \quad \hat{p} = \frac{9}{2} \frac{k}{Q} \frac{m_0}{m} R^5, \quad (9)$$

are two parameters which stand for stellar and planetary tides, respectively. The symbol 0 refers to the star, k_2 is the second degree Love number, Q is the dissipation function or quality factor. It can be shown that the orbital circularization can be accounted by planetary tides only. Indeed, \hat{s} is proportional to $(m/m_0)(1/Q_0)$ which becomes a small quantity for small mass planets and typical stellar Q_0 values. Thus, the contribution of stellar tides can be safely neglected in our analysis (see Rodríguez and Ferraz-Mello 2010).

The timescale for orbital circularization can be defined by $\tau_e \equiv e/|\dot{e}|$, or

$$\tau_e = \frac{3n^{-1}a^5}{7\hat{p}}. \quad (10)$$

Writing Equation (10) as a function of the semi-major axis, we obtain

$$\tau_e = A a^{13/2}, \quad (11)$$

where $A = \frac{3\hat{p}^{-1}}{7\sqrt{Gm_0}}$. Alternatively, we can express the result as a function of the orbital period P in the following way

$$\tau_e = B P^{13/3}, \quad (12)$$

where $B = A \left(\frac{Gm_0}{4\pi^2} \right)^{13/6}$. Figure 10 shows the plot of Equation (12) for a planet with the properties of CoRoT-7b, a Super-Earth planet with $m = 8.5m_E$ (Ferraz-Mello et al. 2011), $R = 1.68R_E$, assuming the values $Q = 100$, $Q = 500$, $Q = 1000$, and $k_2 = 0.35$.

We clearly see that the circularization timescale decreases for short-period planets, as Equation (12) indicates. Moreover, noting that $\tau_e \propto Q$, the orbital circularization would become faster in the case of small Q values (i.e., large dissipation). As an example, for $P = 4$ days and $Q = 100$ we have $\tau_e \simeq 181$ Myr.

It is important to note that the parameter B is linearly dependent on Q/k_2 , which is a quantity poorly known for extrasolar planets. Hence, the plot shown in Figure 10 can be strongly modified if others values of the planet dissipation are considered.

The result (12) can be useful in order to quantify the efficiency of tides to produce orbital circularization of close-in planets. Note that, in some cases, τ_e can be compared with the age of the system, indicating that the orbit of the close-in planet should be circularized during the planet lifetime. However, for large P , τ_e can be even larger than the age of a typical planetary system, in which case a non-circular orbit should be expected due to tidal interaction.

Appendix B: Capture in spin-orbit resonance

The numerical exploration of the planet rotation, which is subject to the gravitational torque of the star, has shown different behaviors including the oscillation around spin-orbit resonances. When a dissipative effect like the tidal torque is included, the rotation can be captured in a resonant motion. The specific capture depends on the eccentricity, and also on Q and ϵ . Hence, as e is tidally damped, the capture should become unstable and the rotation can achieve another resonant state, which, at the same time, should result in a temporary trapping. When the orbit completes the circularization due to the tidal torque, the final evolution result in the synchronization between the orbital and rotational periods (i.e., the 1:1 spin-orbit resonance). The reader is referred to Goldreich and Peale (1966) and Rodríguez et al. (2012) for further details on the spin-orbit evolution of close-in planets.

Let us first consider the torque due to the prolateness or permanent equatorial deformation (i.e., $a \neq b$) on a rotating body of mass m and radius R . The maximum torque, averaged over an orbital period is given by

$$\langle N \rangle = -\frac{3}{2}n^2(B - A)H(p, e) \quad (13)$$

(see Goldreich and Peale, 1966 and Equation (1)), where $H(p, e)$ are power series in e and $p = \Omega/n$, with Ω the angular velocity of rotation of the deformed body (Goldreich and Peale

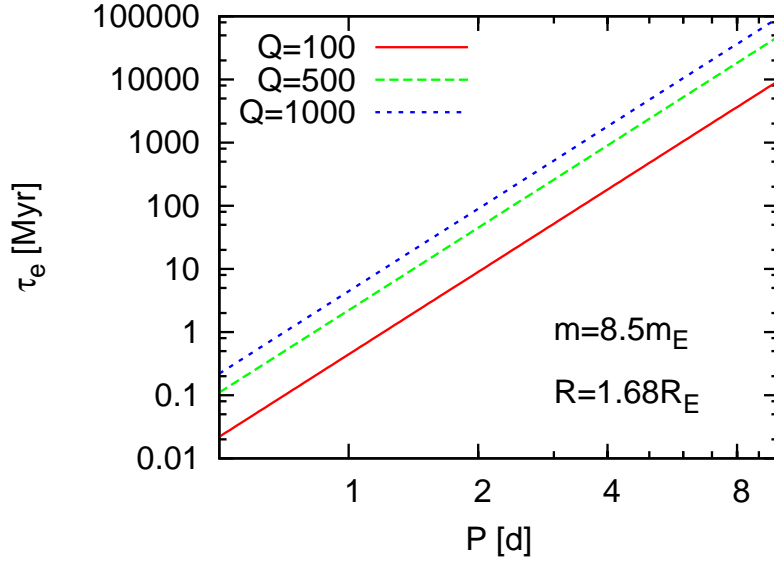


Fig. 10 Plot of Equation (12) for CoRoT-7b super-Earth planet. The mass of the host star is $m_0 = 0.93m_{\text{SUN}}$.

1966). Equation (13) assumes that there is a commensurability between Ω and n , indicating that $p = \dots -1, -1/2, 1, 1/2 \dots$.

In addition to the above torque, we also consider the tidal torque driven by the central body of mass m_0 . The averaged tidal torque reads

$$\langle T \rangle = -\frac{3k_2 G m_0^2 R^5}{8a^6} [4\varepsilon_0 + e^2(-20\varepsilon_0 + 49\varepsilon_1 + \varepsilon_2)] \quad (14)$$

(see Ferraz-Mello et al. 2008), where k_2 is the second degree Love number, whereas ε_i are the phase lags of tidal waves with frequency ν_i . The phase lags account for the internal viscosity, which introduces a delay between the action of the tidal force and the corresponding deformation.

Several tidal models can be used to fix the dependence between phase lags and frequencies, that is, the function $\varepsilon_i(\nu_i)$. We first consider the usually called linear model, where $\varepsilon_i = \nu_i \Delta t$, where Δt is known as time lag and is considered constant in the linear model (Mignard, 1979). The frequencies associated to the phase lags appearing in Equation (14) are $\nu_0 = 2\Omega - 2n$, $\nu_1 = 2\Omega - 3n$ and $\nu_2 = 2\Omega - n$ (see Ferraz-Mello et al. 2008). Replacing into Eq. (14) and applying the linear model, we obtain

$$\langle T \rangle = -\frac{3k_2 \Delta t G m_0^2 R^5 n}{2a^6} [2p - 2 + (15p - 27)e^2]. \quad (15)$$

The time lag can be related to the most used quantity Q , the dissipation function. Since $\varepsilon_i \simeq Q_i^{-1}$, it follows, under assumption of linear model, $Q_0^{-1} \simeq 2n\Delta t(p-1)$, $Q_1^{-1} \simeq n\Delta t(2p-3)$, $Q_2^{-1} \simeq n\Delta t(2p-1)$. We note that singularities in Q_i are associated to spin-orbit commensurability with $p = 1$, $p = 3/2$ and $p = 1/2$. Since we restrict our investigation to the cases of 1:1 and 3:2 spin-orbit resonances, we call $Q = Q_2$ in order to avoid Q_i -singularities. Hence, the relationship between Q and Δt is given by $Q = 1/[n\Delta t(2p-1)]$.

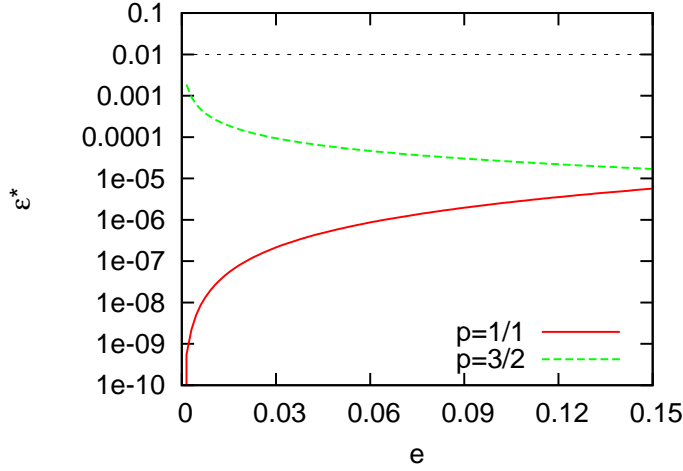


Fig. 11 Critical value of the equatorial ellipticity as a function of orbital eccentricity for two spin-orbit resonances. The CoRoT-7+7b system illustrates the example.

Stationary solutions

By definition, the stationary solutions of the rotation are those which satisfy

$$\langle N \rangle + \langle T \rangle = 0. \quad (16)$$

Because we are interested in those solutions for which there exist commensurability between spin and orbital revolutions, we can determine a critical value of ϵ (we call it ϵ^*) which allows a spin-orbit resonance motion be maintained when the planet's rotation is under simultaneous action of two torques. Thus, using Equation (13,15,16) we obtain

$$\epsilon^* = -\frac{1}{\xi} \frac{k_2}{Q} \frac{m_0}{m} \left(\frac{R}{a}\right)^3 \frac{[2p - 2 + (15p - 27)e^2]}{(2p - 1)H(p, e)}. \quad (17)$$

where we have used the third Kepler law and $(B - A) \simeq C\epsilon = \xi m R^2 \epsilon$, where C is the moment of inertia about the rotation axis and $0 < \xi \leq 2/5$.

The condition $\epsilon > \epsilon^*$ is usually known as stability condition of the p -resonance (e.g. Goldreich, 1966). In fact, the stability condition requires that $\langle T \rangle$ not exceed the maximum restoring torque $\langle N \rangle$ and, for that reason, ϵ^* should be considered as a critical value.

We note that the case $p = 1$ is in agreement with the result found in Ferraz-Mello et al. (2008) for the synchronous motion¹⁴.

Figure 11 shows the variation of ϵ^* with the orbital eccentricity, taking the planet CoRoT-7b as an example. We adopt $k_2 = 0.35$, $\xi = 0.35$ and $Q = 100$. The cases of 1 : 1 (synchronous rotation) and 3 : 2 spin-orbit resonances are shown. To second order in eccentricity, we have $H(1, e) = 1 - 5e^2/2$ and $H(3/2, e) = 7e/2$. The dashed horizontal line indicates the value of ϵ used in the simulations for CoRoT-7b ($\epsilon = 0.00992$; Figures 2(a,b)). We note that $\epsilon > \epsilon^*$ in both cases, indicating that the resonant motion should be stable for the range of considered eccentricity. However, ϵ^* can reach high values for very small e as Equation (17) indicates. On the other hand, we have seen in the numerical simulations (no tides case, Figure 2(b)) that the domain of the 3 : 2 spin-orbit resonance is very small for almost-circular orbits.

¹⁴ For comparison it is necessary to consider the relationship between J_{22} (the equatorial ellipticity) and $B - A$, that is, $B - A = 4J_{22}mR^2$ (see Beutler 2005).